


Article

Multi-Layer Ceramic Capacitors in Lighting Equipment: Presence and Characterisation of Rare Earth Elements and Precious Metals

Konstantinos M. Sideris ^{1,2,*}, Dimitrios Fragoulis ³, Vassilis N. Stathopoulos ³  and Panagiotis Sinioros ¹

¹ Department of Electrical & Electronic Engineering, University of West Attica, 122 44 Egaleo, Greece; pasin@uniwa.gr

² Department of Electrical and Electronic Engineering Educators, School of Pedagogical and Technological Education, 151 22 Marousi Attica, Greece

³ General Department of National, Kapodistrian University of Athens, 344 00 Evia, Greece; dimifragkoulis@uoa.gr (D.F.); vasta@uoa.gr (V.N.S.)

* Correspondence: ksideris@uniwa.gr

Abstract: The need to reduce energy consumption in buildings, the emergence of light-emitting diode (LED) lamps in lighting around 2010, their long lifetime, and the 2025 target to use only LED lamps are changing the existing composition of Category 3 waste electrical–electronic equipment (WEEE) and creating expectations for simple, high-concentration recycling streams. In this study, multi-layer ceramic capacitors (MLCCs) detached from the lighting sector’s WEEE were characterised for the presence of rare earth elements (REEs) and precious metals (PMs). Their digestion was carried out with HNO₃ and aqua regia on a heating plate and characterised using inductively coupled plasma optical emission spectroscopy (ICP-OES) and scanning electron microscopy with energy-dispersive X-ray spectroscopy (SEM-EDX). The contents of REEs and PMs found in the MLCCs were 0.84 wt% and 0.60 wt%, respectively, and create an economic stored value that is essentially defined by PMs of 98.67% and by palladium (Pd) of 78.37%. The analysis showed that the content of the main elements was: neodymium (Nd) 0.366 wt%, yttrium (Y) 0.220 wt%, dysprosium (Dy) 0.131 wt%, silver (Ag) 0.467 wt%, and Pd 0.105 wt%. These results indicate the need for selective removal and separate recycling processes of MLCCs from WEEE drivers.

Keywords: measurements and characterisation; lighting equipment; multi-layer ceramic capacitors; rare earth elements; precious metals; inductively coupled plasma optical emission spectroscopy (ICP-OES) analysis



Citation: Sideris, K.M.; Fragoulis, D.; Stathopoulos, V.N.; Sinioros, P. Multi-Layer Ceramic Capacitors in Lighting Equipment: Presence and Characterisation of Rare Earth Elements and Precious Metals. *Recycling* **2023**, *8*, 97. <https://doi.org/10.3390/recycling8060097>

Academic Editors: Dechao Hu and Zhixin Jia

Received: 29 September 2023

Revised: 13 November 2023

Accepted: 19 November 2023

Published: 4 December 2023



Copyright: © 2023 by the authors. Licensee MDPI, Basel, Switzerland. This article is an open access article distributed under the terms and conditions of the Creative Commons Attribution (CC BY) license (<https://creativecommons.org/licenses/by/4.0/>).

1. Introduction

Electrical–electronic equipment (EEE) at the end of its life is characterised as waste electrical–electronic equipment (WEEE) or, more simply, electronic waste (e-waste) and classified into one of its categories according to the European Union (EU) Directive 2012/19. Environmental protection and natural resource preservation require equipment recycling. E-waste includes at least 57 elements of the periodic table, some of which have significant economic value. Therefore, e-waste can be used as an important secondary source of base metals (BMs), special metals, rare earth elements (REEs), precious metals (PMs), glass, plastic, and functional structures–components, which can be reused in equipment production or repair [1–4].

REEs include lanthanides, scandium (Sc), and yttrium (Y), while PMs include platinum group metals, gold (Au), and silver (Ag). Generally, lanthanides include lanthanum (La), cerium (Ce), praseodymium (Pr), neodymium (Nd), promethium (Pm), samarium (Sm), europium (Eu), gadolinium (Gd), terbium (Tb), dysprosium (Dy), holmium (Ho), erbium (Er), thulium (Tm), ytterbium (Yb), and lutetium (Lu). PGMs include the elements

ruthenium (Ru), rhodium (Rh), palladium (Pd), osmium (Os), iridium (Ir), and platinum (Pt). Rare earth elements and precious metals are identified by the EU (2023) as critical raw materials (CRMs) and are accompanied by the indicators of “supply risk” (SR) and “economic importance” (EI). A vast number of these elements make their recovery from e-waste, which poses a significant recycling challenge [5–10].

The presence of the abovementioned elements has a different impact on EEE versus WEEE. More specifically, in the first case, they improve the energy efficiency and enhance its protection from environmental effects, while in the second, due to higher and cleaner concentrations, they boost the idea of “urban mining” through the recycling–recovery process and simultaneously counteract natural reserve exhaustion (the balance problem). In particular, the presence of significant quantities of precious metals with a high economic value supports the effort to recover them from urban mines and the viability of recycling plants. It is worth noting that, for the year 2019, the stored mass of specific precious metals in e-waste corresponded to Ag 1200 t, Au 200 t, Ir 1 t, Ru 0.3 t, and Pd 100 t [2,11–20].

To investigate the recoverability of CRMs and whether it is cost-effective to do so, the characterisation of e-waste and the mapping (identification) of CRMs in the various structures and components of the equipment are required beforehand.

1.1. Characterisation of E-Waste for the Presence and Quantity of REEs and PMs

For the characterisation of e-waste (structures–components), regarding the presence and quantity of specific elements, destructive or non-destructive methods can be employed, such as multi-scale electron microscopy techniques based on reflection/transmission modes (SEM, TEM) coupled with energy-dispersive X-ray spectroscopy tool options (EDX). Additionally, X-ray fluorescence (XRF), microwave plasma atomic emission spectroscopy (MP-AES), thermogravimetric analysis (TGA), inductively coupled plasma optical emission spectroscopy (ICP-OES), inductively coupled plasma atomic emission spectroscopy (ICP-AES), and inductively coupled plasma mass spectrometry (ICP-MS) may also be used. Method choice is a crucial parameter that affects the final analysis. The choice considers essential parameters related to the sample, such as (a) type, (b) structure, (c) construction materials, and (d) concentrations. For low concentrations, plasma-related methods, e.g., ICP-OES and ICP-MS, are selected that can detect extremely low concentrations [8,21–28].

1.2. Recycling of E-Waste for the Recovery of REEs and PMs

During the recycling process of e-wastes, the pre-treatment stage aims at (a) their separation and dismantling; (b) the removal of “hazardous” parts that need special handling; (c) the separation of structures–components based on their functionality; (d) selective removal of components (“look and pick”), based on the concentrations of specific valuable metals or critical raw materials; (e) the creation of recycling flows with simple compositions and high concentrations; (f) minimisation of critical raw material losses and the improvement of recovery; (g) the sustainability of recycling plants; (h) the ideal balance between the economic benefit of recycling and the reduction of its environmental footprint [3,8,9,12,21,29–32].

1.2.1. Separation and Dismantling

Separation of E-Waste

The separation of waste electrical and electronic equipment starts at the collection point. Separating equipment is particularly important because it prevents it from being contaminated with hazardous waste, including the mercury contained in fluorescent lamps. According to Directive 2012/19/EU, and in particular as of 2019, WEEE is divided into six categories: (Category 1) temperature control equipment; (Category 2) monitors, displays, and equipment containing monitors with a surface area greater than 100 cm²; (Category 3) lamps; (Category 4) large equipment (any external dimension greater than 50 cm); (Category 5) small equipment (no external dimension greater than 50 cm); (Category 6) small IT and

telecommunications equipment (no external dimension greater than 50 cm). It should be noted that the categories of e-waste differ between countries and continents [32].

Separation between Each Category of E-Waste

Separation of WEEE within the same category can be used for equipment that operates according to a different principle and, therefore, has a different composition; for example, different lamp technologies. Recycling streams with a simpler composition result from this separation. For possible repair and reuse, the equipment's functionality is also considered.

1.2.2. Dismantling

Dismantling of E-Waste

During the dismantling phase, the e-waste components that are hazardous to the environment and human health are removed, and the drivers of the equipment and the remaining parts are separated, usually into metal, plastic, glass, etc. The removal of structures and components requiring special treatment, as well as drivers, screens, etc., is usually performed manually.

The remaining parts of the equipment can be sent to special shredders to reduce the size of their structures. After shredding, special equipment is used to separate them into different fractions (plastic, metal, etc.), enriching recycling streams. The technologies used for enrichment are (a) air separation, (b) gravity separation, (c) magnetic separation, (d) electrostatic separation, and (e) froth flotation [32].

Dismantling of Specific Structures of E-Waste (Electronic Drivers)

Driver disassembly aims to remove components that require special treatment, such as electrolytic capacitors and batteries. The remaining components are separated according to their elemental composition. The disassembly process can be carried out either manually or automatically. The separation of components can be performed macro-optically by manual separation or by using different technologies. These technologies usually use the components' shape, colour, and magnetic properties [33,34].

1.3. E-Waste and Electronic Drivers

Electrical–electronic equipment usually includes or is accompanied by drivers (Figure 1a,b) responsible for its proper operation. Not only from a functional point of view but also from a recycling point of view, drivers constitute an important or possibly the EEE's most important structure [3,35]. Depending on the type of equipment, their percentage weight differs significantly (~2–30%) without this being an indication of its stored economic value. A conventional driver consists of a printed circuit board (PCB) and electrical–electronic components (EECs), which are divided into through-hole components (THCs) and surface mount devices (SMDs). Drivers may include multi-layer ceramic capacitors (MLCCs), usually in SMD form. Their number and total mass are considered a function of the circuit's electronic design and the PCB's layout. Using capacitors of this type in the design and construction of drivers offers numerous advantages, such as minimal dimensions, reliability, and a lack of polarity [13,15,16,25,27,36–39].

Multi-Layer Ceramic Capacitors (MLCCs)

Multi-layer ceramic capacitors consist of the main body and terminals (Figure 2a). The main body incorporates metal electrodes and a ceramic dielectric (Figure 2b,c). Usually, terminals are formed by three layers (the substrate, barrier, and external layers) (Figure 2d). Ni, Sn, Cu, Ag, Pd, and Pt, in single or compound form, are used to manufacture electrodes and terminals.

Formerly, Ag and Pd were primarily used to manufacture these structures of capacitors. In the last thirty years, the significant cost increase in their production has led to a technological shift from precious metals to base metals, thus creating BMs-MLCCs. Today, the share of BM-MLCC nickel (Ni) accounts for 60% of the total production of MLCCs.

Despite the above treatment, there is ongoing scientific interest in creating new materials to eliminate the use of precious and critical metals for cost reduction and mitigate the “balance problem” [3,13,22,27,40–44].

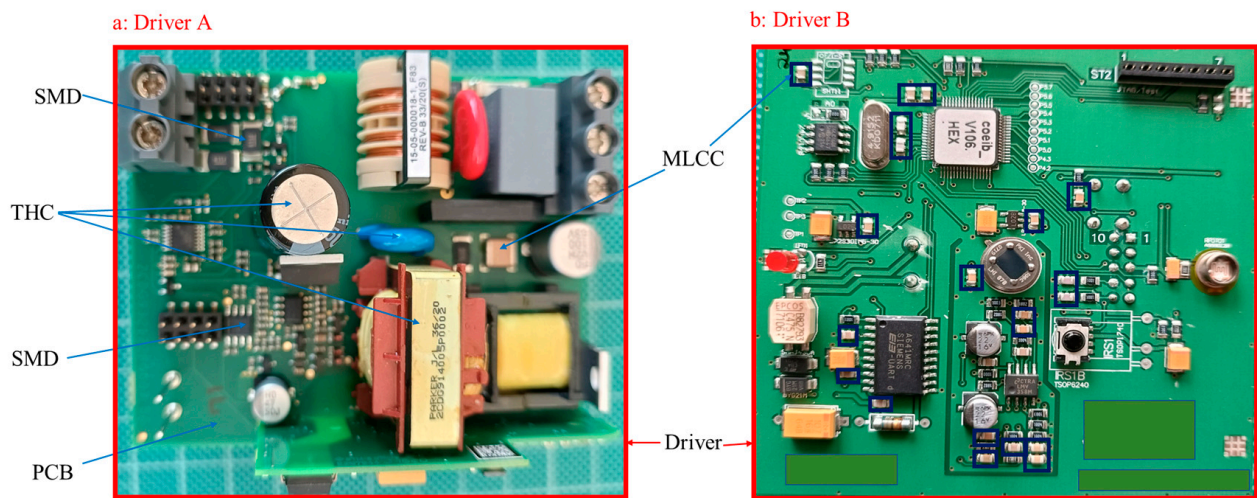


Figure 1. Indicative driver structures and their components. Drivers A and B belong to different lighting management equipment (Authors’ images).

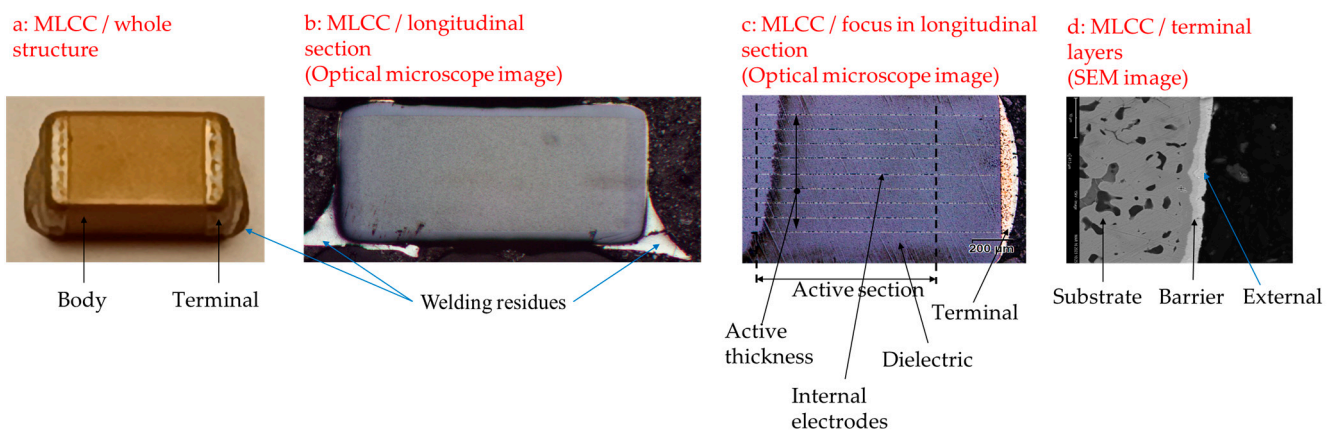


Figure 2. An indication of the external and internal structure of MLCCs (Authors’ images).

This technological shift led to a deterioration in MLCCs’ critical parameters. Since precious metal concentrations were diminished, the durability of capacitors was negatively affected, leading to a reduction in the equipment’s service life. From a recycling point of view, this change was accompanied by valuable material contents that gradually declined throughout the years [37,44,45]. The challenges in their design, dictated by the requirement for high capacity in a small volume and less precious metal use, have been achieved by using rare earth elements as impurities in forming the ceramic dielectric (usually BaTiO_3). The adoption of these elements led to (a) excellent properties related to the dielectric constant (high- k), dielectric losses (low $\tan\delta$), and electrical properties even for thin dielectric layers ($<1\ \mu\text{m}$); (b) high performance and reliability of base metal electrode (BME) nickel capacitors while maintaining reduced production costs; and (c) the inclusion of ceramic dielectrics in their design and production [27,46–52]. Many elements in e-parts hinder their recoverability, mainly when their concentrations are extremely low. MLCCs’ characterisation, separation, and separate recycling make their content recovery more effective, contributing to natural resource conservation and the electronic industry’s partial independence from CRM mining and commercialisation monopolies [4,10,28].

1.4. Artificial Lighting and MLCCs

The recent entry (2010) of LED technology into the building lighting sector, the continuous increase in their share of the lighting market, their long-rated lifetime, and the need for the implementation of zero-energy buildings (ZEBs) and zero-energy homes (ZEHs) create a new composition of specific e-wastes that require separate streams for their recycling. Lighting equipment (LE) maintains an inner lighting intensity at a desired level and saves building energy. Depending on its type and specifications, lighting equipment may contain multi-layer ceramic capacitors. MLCC palladium's remarkable concentration adds stored value to drivers in such a case. Mainly due to the Pd concentration, capacitors of this type are characterised as "target components" among other electrical–electronic components of the driver for its selective removal and separate recycling process [16,18,40,44,45].

It is worth mentioning that only a few studies related to the removal and characterisation of multi-layer ceramic capacitors from the drivers of specific e-wastes are available [40,53]. Based on the literature review, twelve studies were identified to be related to their characterisation, while only six concerned specific capacitors or capacitors from specific e-wastes. In particular, capacitors from computers were used by [53]; specific colour components were used by [8]; non-magnetic components were used by [45]; personal computers were used by [40]; X7R-0603 BME-MLCCs were used by [25]; and Ni-rich MLCCs were used in [26,41].

The novelties of this study can be summarised by the presence of multi-layer ceramic capacitors in specific lighting equipment coupled with the identification and quantification of REEs and PMs in MLCCs. Data derived from this endeavour can be utilised to suggest new recycling protocols for efficiently recovering these metals.

2. Materials and Methods

2.1. Materials

This study used the following lighting equipment: (a) light management equipment (LME) corresponding to a 240 m² house, (b) lamp and luminaire light-emitting diode (LED) technology, and (c) external drivers for LED strips. The above equipment differed in terms of electrotechnical–photometric characteristics and brand name (BN) and was provided by: (a) AEGEAN RECYCLING-FOUNDRIES SA (lamps, luminaires, and drivers), (b) FEILO SYLVANIA GREECE SA (lamps), and (c) ABB Greece and SIEMENS Greece (LME).

2.2. Methodology

The methodological approach followed in this study included six stages: (1) collection and separation, (2) disassembly and testing, (3) sample preparation, (4) ICP-OES analysis, (5) EDX analysis, and (6) SV calculation. To assist the reader, a colour guide is provided in Figure A1. Also, a detailed description of the laboratory steps from the collection of lighting equipment to the characterisation of MLCCs is presented in Figure A2. All measurements were repeated three times under the same conditions, and the results were averaged.

2.2.1. First Stage—Collection and Separation

The first stage involved the collection, cleaning, visual integrity checking, and separation of the equipment according to (a) the e-waste categories, (b) its use (domestic or professional), and (c) the LED technology (surface mount device or filament) (Figure A3). The lighting equipment corresponded to three categories of e-waste: Category 3 (lamps), Category 4 (large equipment), and Category 5 (small equipment). In this study, the addition of Index C to LED lamps indicates that they are lamps containing surface mount device LEDs (SMD LEDs), while the addition of Index R indicates that they refer to lamps containing filament LEDs. For example, the type of lamp is E27 and is modified to E27-C and E27-R.

2.2.2. Second Stage—Disassembly and Testing

The second stage involved initial weighing of the equipment, complete manual disassembly, and the weighing of its structures and components for the correlation between its masses using basic and special tools such as magnifying glasses, precision tweezers, the hot air-gun rated temperature (brand, BOSCH; (Robert Bosch GmbH, Stuttgart, Germany) model, GHG 20-60), balances (brand, Kern; (KERN & SOHN GmbH, Balingen, Germany) model, EMB 3000-1, $d = 0.1$) (brand, KERN; (KERN & SOHN GmbH, Balingen, Germany) model, EHA 1000-1, $d = 0.1$), and a precision balance (brand, KERN (KERN & SOHN GmbH, Balingen, Germany); model, EWJ-300-3, $d = 0.001$ g). For the reliability of the samples, and because the exterior of SMD inductors resembles MLCCs, in addition to the macroscopical control during the removal of multi-layer ceramic capacitors from the drivers, their digital control was performed piece-by-piece to exclude the possible presence of SMD inductors between them using a digital instrument identifier for surface mount device components (brand, Mastech; (MGL International Group Limited, Taipei, Taiwan) model: MS8910). MLCCs were counted and weighed for each item of equipment to generate innovative data on their presence in it. Finally, before their magnetisation check [54], a representative sample was removed for EDX analysis, while the remaining capacitors were examined using a Nd magnet for the initial quantitative assessment of precious metals in their structure according to the methodology followed in [45].

2.2.3. Third Stage—Sample Preparation

To eliminate any possible organic composition on the examined multi-layer ceramic capacitors (e.g., conformal coating), the samples were burned at 700 °C. Because of this, the third stage involved the preparation of the porcelain crucibles (brand, JIPO; (Jizerská porcelainka sro, Desná v Jizerských horách I, Czechia) form, middle) to investigate the difference in mass of the samples before and after their burning using an analytical balance (brand, KERN; model, ABP 200-4M, $d = 0.0001$), a laboratory oven (brand, THERMOLYNE; (THERMOLYNE–ThermoFisher Scientific, Waltham, MA, USA) model, 30,400), and a desiccator. To burn samples more efficiently and avoid contamination, slight breaking of the capacitors was carried out in an agate mortar. Potential mass loss was tested using an analytical balance (brand, SHIMADZU (SHIMADZU Corporation, Kyoto, Japan); model, AUX320, $d = 0.0001$) and the difference was negligible. The temperature and time profiles are presented in Figure 3.

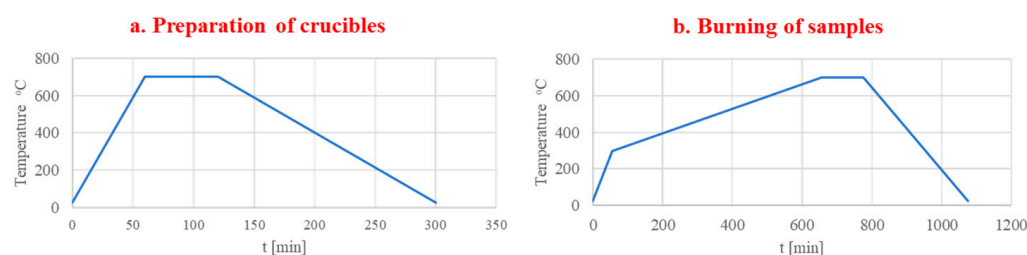


Figure 3. Temperature and time profiles: (a) preparation of crucibles and (b) burning of MLCCs.

2.2.4. Fourth Stage—ICP-OES Analysis

The fourth stage involved the pulverisation of capacitors to create laboratory samples (quartering, ~1 g per sample) and make the most effective approach to acids in samples according to the methodology followed in [1,24,40] using a ball mill (brand, FRITSCH (FRITSCH GmbH, Idar-Oberstein, Germany); model, pulverisette 6) with a zirconium oxide planetary ball mill tank (brand, FRITSCH; volume, 80 mL), and an analytical balance (brand, SHIMADZU; model, AUX320, $d = 0.0001$). Digestion of the samples was carried out in glass beakers with a solid–liquid ratio of 1:40 and on a heating plate at 90–100 °C by manual stirring for a period of 3 h or for as long as required for their digestion. Their digestion was carried out in a chemical fume hood, implementing personal and environmental protection regulations.

The determination of Ag and REEs was carried out in nitric acid (HNO_3) and the determination of the remaining PMs was carried out in aqua regia ($\text{HCl}:\text{HNO}_3$, ratio: 3:1) according to the methodology followed in [8,21,31] using the acids HNO_3 65% and HCl 35–38% (all analytical grade; brand, MACRON (MACRON-avantior, Pennsylvania, PA, USA); purchased from Chemix SA), according to the methodology in [1,8,15,55,56]. Calibration of the ICP-OES instrument was carried out using ICP calibration standards: (a) REEs (brand, CPA hem (Bogomilovo, Bulgaria); name, MISA Standard 1—Rare Earth Metals—18 components), (b) PMs (except for Ag), (brand, CPA hem; name, MISA Standard 2—Precious Metals—6 components), and (c) Ag (brand, hps; name, ICP-AM-MISA6—27 component). Filtration of solutions to protect the ICP-OES instrument was carried out using filter paper (brand, Ahlstrom-Munksjö (Ahlstrom Group, Helsinki, Finland); type, Hardened Low-Ash Grades: 391) and ultrapure water (brand, PanReac; (PanReac AppliChem, Castellar del Vallès, Barcelona type, LC-MS). ICP-OES solution analysis was carried out to quantify REEs and PMs in samples according to the methodology followed in [27,53] using the ICP-OES instrument (brand, Agilent (Agilent, Santa Clara, USA); model, 5110).

The ICP-OES instrument was calibrated using five aqueous standard solutions (0.5, 2, 4, 10, and 20 (mg L^{-1})) for REEs and PMs except for Pm and Os. The operating parameters of the ICP-OES instrument were the same for HNO_3 and aqua regia: radio frequency power, 1300 W; nebulization gas flow, 0.8 (L min^{-1}); auxiliary gas flow, 0.2 (L min^{-1}); plasma gas flow, 15 (L min^{-1}); sample aspiration rate, 1.5 (L min^{-1}); torch configuration, axial.

2.2.5. Fifth Stage—SEM-EDX Analysis

The fifth stage involved the SEM-EDX analysis of nine multi-layer ceramic capacitors. The capacitors were encapsulated in conductive resin, and their longitudinal sections were subjected to friction and polishing according to the methodology followed in [57] using a grinding and polishing machine (brand, Struers (Struers S.A.S., Champsigny sur Marne cedex, France); model, rotopol 35). An optical microscope (brand, ZEISS (Carl-Zeiss, Oberkochen, Germany); model, HAL 100 with an OLYMPUS DP22 camera) and an SEM-EDX (brand, Thermo Scientific (ThermoFisher Scientific, Waltham, MA, USA); model, Phenom XL) were employed in this study.

2.2.6. Sixth Stage—Calculation of Stored Value

The stored value due to the presence of rare earth elements, precious metals, and their percentage distribution at an assumed mass of 1 kg of MLCCs from lighting equipment was calculated by considering only their usable concentrations from the ICP-OES analysis results and their current market prices.

3. Results and Discussion

3.1. Estimation of the Chronology of Lighting Equipment

The LE manufacture date is essential information for the recycling sector for two main reasons. Firstly, the concentrations of e-waste are linked to the manufacturing technology of the respective period, and the PM and REE concentrations change over time. To estimate the chronology of the LE collected in 2021, the following parameters were taken into account: (a) the protocol EU-1194/2012 for determining the lifetime of LED lamps, (b) the Directive 2009/125/EC and the Regulations 244/2009 and 1194/2012, (c) the efficiency (lm W^{-1}) of the examined lamps and luminaires compared to their new-type counterparts (Figure A4) concerning the “net zero scenario” 2010–2030 to improve their performance ($\sim 4 \text{ lm W}^{-1}$ per year), (d) the average lifetime specified by the manufacturer, (e) the effects of temperature on the photometric and electrotechnical characteristics of lamps as a function of luminaire types, (f) various imponderables, such as the failure of materials and components and power line grid surges, and (g) average daily operation of six hours for household lamps and twelve hours for professional equipment (lamps and luminaires) according to Commission Regulation-EU 1194/2012/ ANNEX II [58–65].

Considering the abovementioned parameters, it was estimated that the manufacturing date of the examined LED lamps and luminaires was between 2016 and 2021. Based on matching current equipment and sponsor information, the manufacturing date of the external LED drivers is between 2018 and 2021 and that of the LME is between 2012 and 2020.

3.2. MLCCs in Lighting Equipment

The experimental and computational results for each tested type of lighting equipment are presented below. More analytically, the variation in the total mass per type of lighting equipment and the variation in the mass percentage between the driver and LE are presented in Figures 4 and 5, respectively. The variation in the mass of LE drivers falls within the variation of (~2–30%) among the WEEE drivers, except in the cases of ELEDDCT and LME. External LED drivers, the semi-closed type, and the G9-R and R7S-R LED lamps had no multi-layer ceramic capacitors and thus were not investigated further. The absence in the first type is due to the driver's electronic design, whereas in the other two no driver is required. The probability of the presence (existence) of MLCCs in each sample by type of lighting equipment tested is shown in Table 1. For example, GU10 (48%) means that some lamps contained MLCCs, while the rest (52%) did not have MLCCs in the driver. The variation in the mass of the MLCCs as a percentage of the mass of the driver in the LE is shown in Figure 6, where their percentage in the G9-C lamps is huge in comparison with the rest of the equipment.

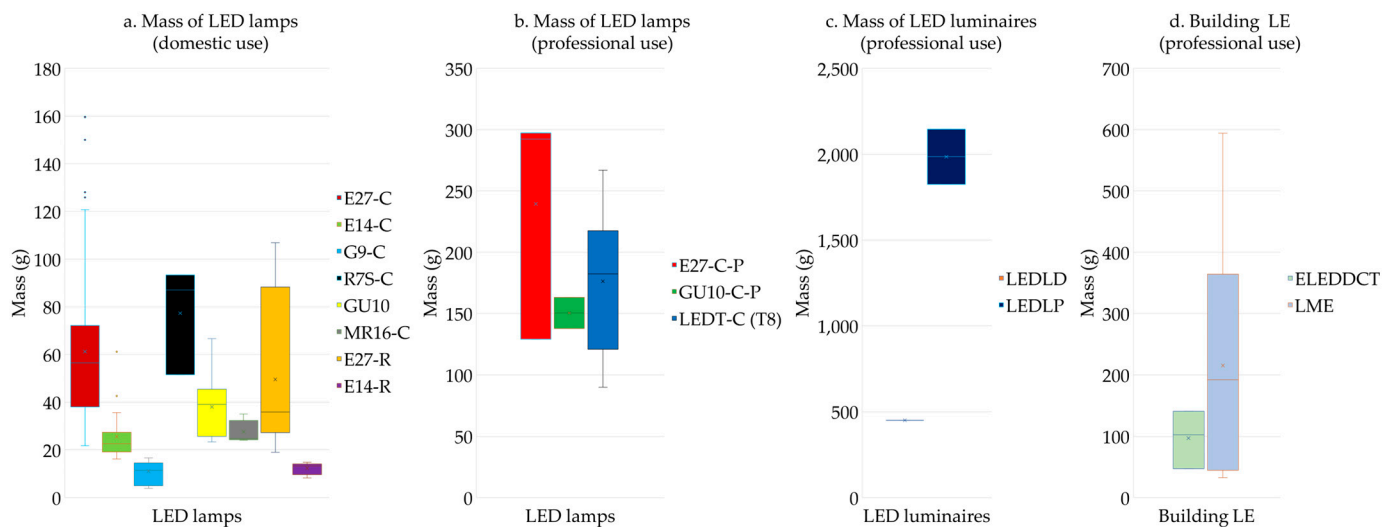


Figure 4. Mass variation in the different types of LE under investigation in this study.

Table 1. Percentage presence of MLCCs in LE used in this study.

E27-C	E14-C	G9-C	R7S-C	GU10	MR16	E27-R	E14-R	E27-C-P	GU10-C-P	LEDT (T8)	LEDLD	LEDLP	ELEDDCT	LME
66%	65%	57%	100%	48%	100%	55%	13%	67%	100%	38%	100%	100%	67%	100%

The presence and their number for each type of electrical–electronic equipment are inter-related concepts. In particular, the LE's capacitors are significantly smaller than their corresponding number in other e-wastes. More thoroughly contained are LED lamps 1–7, LED luminaires 2–7, closed-type external LED driver (ELEDDCT) 9, and LME 9–60.

On the other hand, their number in specific equipment corresponds approximately to: TV sets 300, LED TVs and personal computers greater than 1000, personal digital assistants 200, and mobile phones 150–200. Smartphones are the type of equipment with the highest

demand for these capacitors between the EEE, with their number depending on their BN and specifications and changing significantly [18,22,24,37,40,50,66]. According to [40], drivers have a multitude of these capacitors in their structure. In [30], it was reported that, in a classic hybrid driver design, their number, as a percentage versus the number of EECs, corresponds to about 30%. The recycling sector focuses on the presence and total mass of capacitors as a function of the types of e-waste. The variation in capacitors' mass per examined lighting equipment type is shown in Figure 7a, highlighting G9-C lamps as the most efficient type with a value that coincides with the maximum of the total configuration that ranged between 0.033 and 0.328 g. It has been taken into account that there is no study related to the calculation or estimation of MLCCs' total mass and that there are no valid results to compare. Each of the included capacitors differs in mass and is characterised by an average mass-per-piece (MpP) value for each type of examined lighting equipment (Figure 7b).

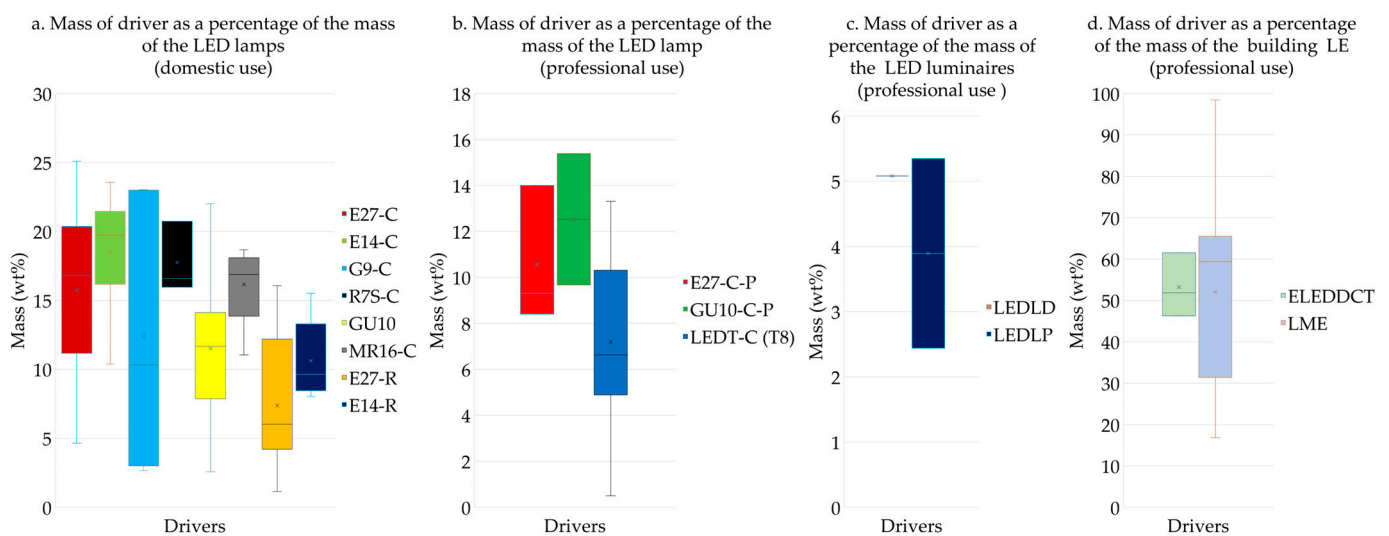


Figure 5. The mass variation in the driver as a percentage of the mass of the LE used in this study.

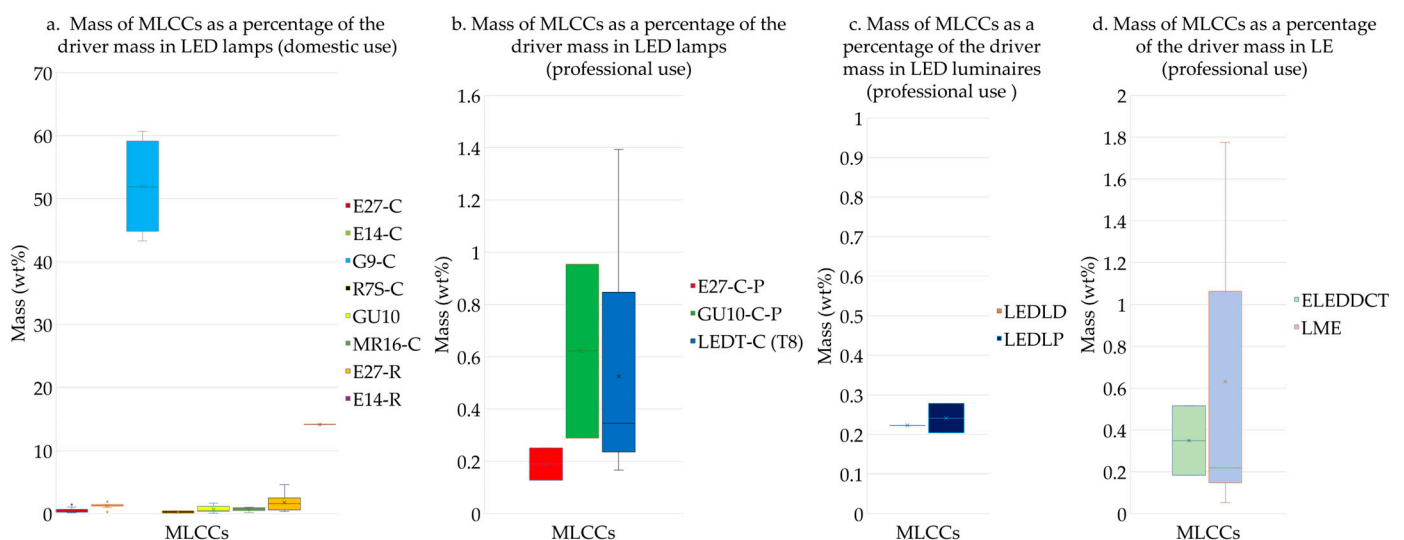


Figure 6. Variation in the mass of the MLCCs as a percentage of the mass of the driver in the LE used in this study.

How high or low the MpP factor is determines the profitability of their manual extraction from drivers. The mass-per-piece value stems from the division of their total mass. MLCCs with different MpP factors are shown in Figure 8.

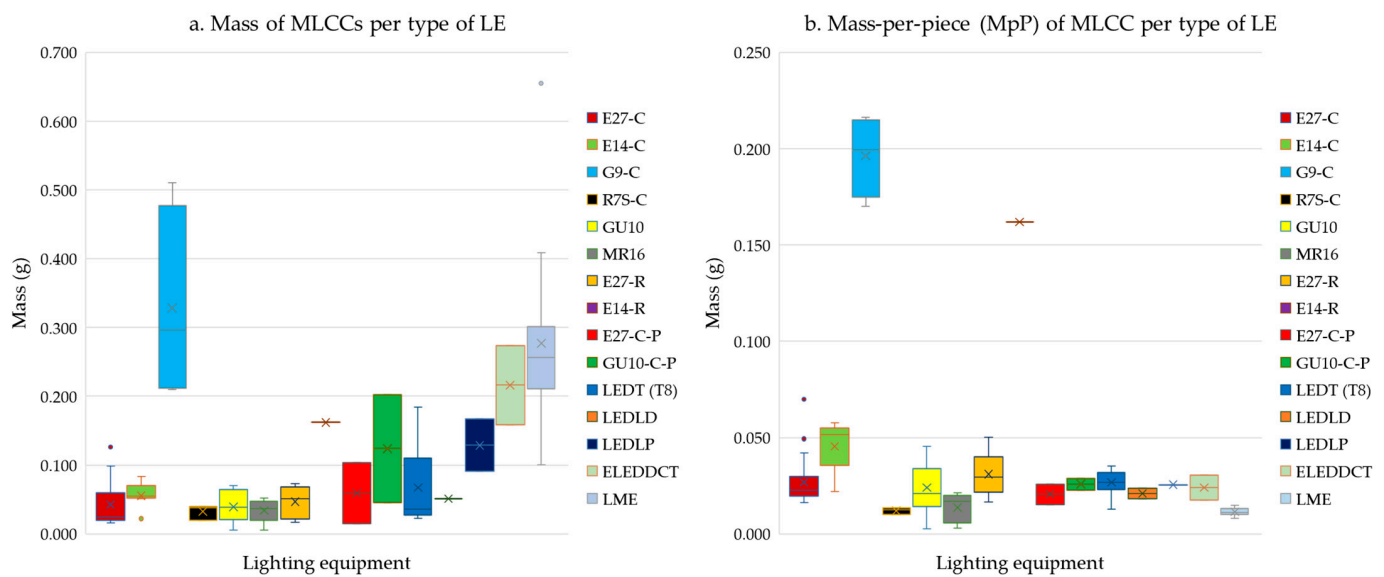
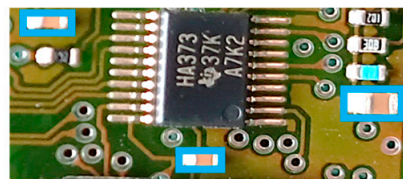


Figure 7. (a) Variation in the total mass of the capacitors as a function of the type of equipment tested. (b) Variation in the MLCC piece weight factor with the type of LE tested.

a. Selected area of a driver from LME



b. Driver from G9-C LED lamp

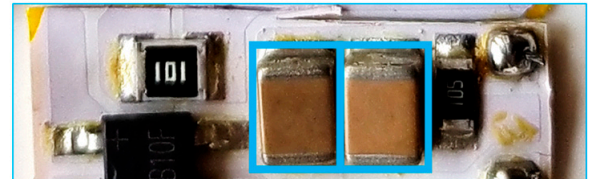


Figure 8. MLCCs with different mass-per-piece indices (Authors' images).

The presence of encapsulated drivers, and depending on the encapsulation material, makes the release of EECs extremely difficult (Figure 9). The presence of encapsulated drivers focused on four types of lamps with their respective percentages per lamp type examined: (a) E27-C (6.78%), (b) GU10 (8.00%), (c) MR16 (20.00%), and (d) R7S-C (100%).

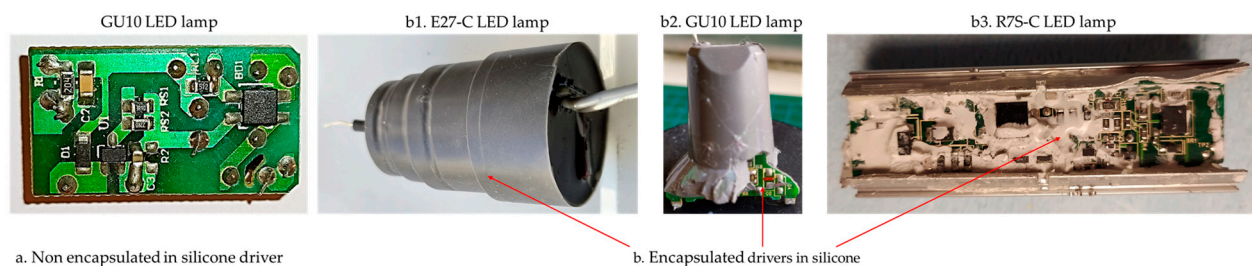


Figure 9. (a) Non-encapsulated drivers. (b) Drivers encapsulated in silicone (Authors' images).

For the characterisation of each examined LE for the collection of the mass of MLCCs, from an assumed mass 1 (t) of each examined LE, the following equipment parameters were taken into account: (a) the mass of each type of LE (Figure 4); (b) the percentage presence of MLCCs in LE (Table 1); (c) the mass of MLCCs per type of LE (Figure 7a); (d) the MpP factor per type of LE (Figure 7b); and (e) the number of each type of LE for the assumed mass of 1 t (Figure 10).

The calculated results highlight LED lamp G9-C as the most advantageous type among the lighting equipment used in this study for the collection of multi-layer ceramic capacitors (Figure 11).

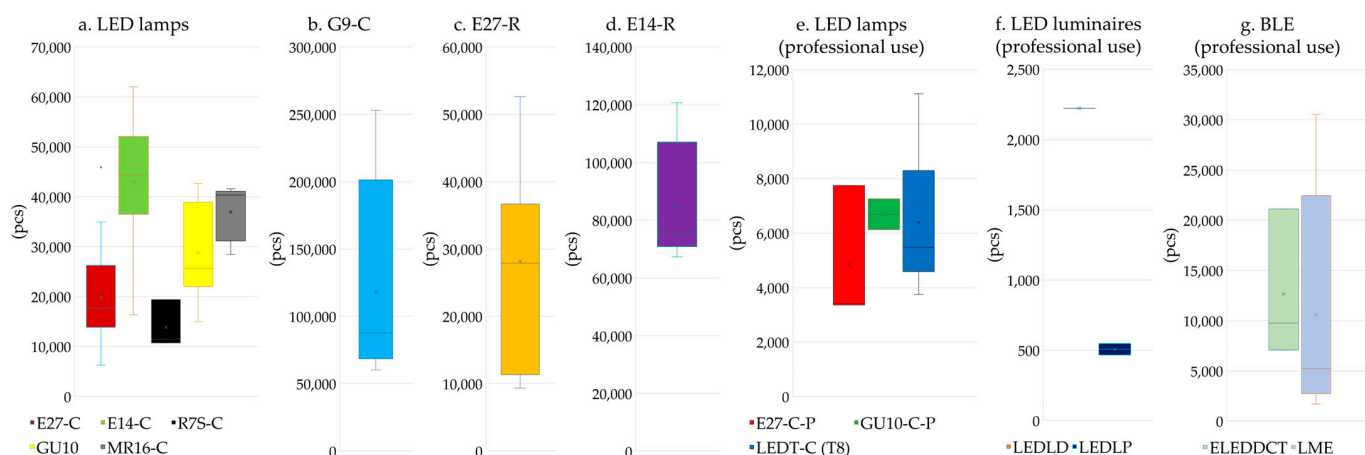


Figure 10. The number of pieces of each type of lighting equipment used in this study per 1 tonne of each type of lighting equipment.

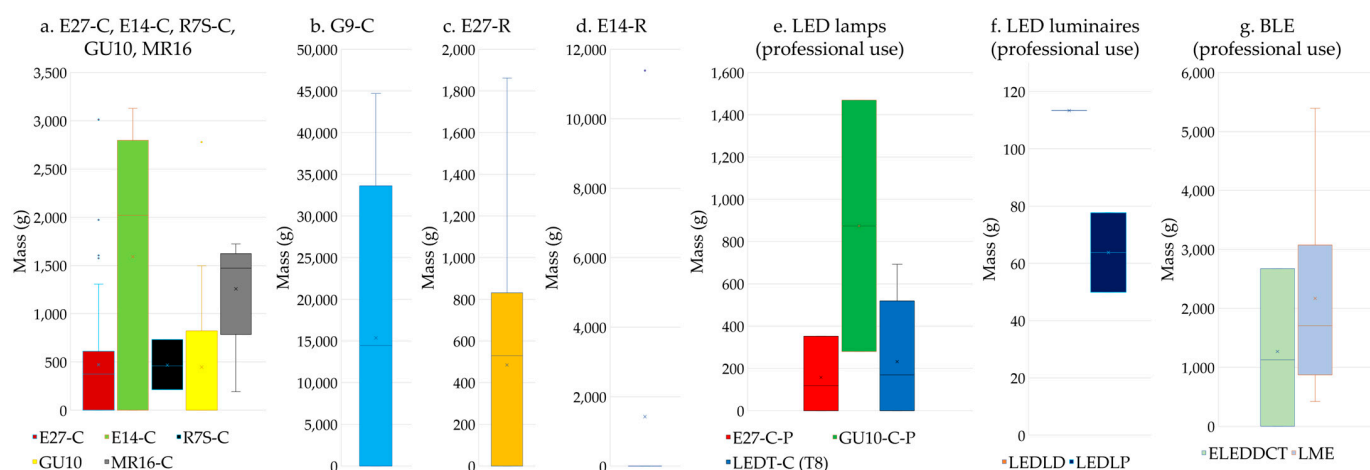


Figure 11. Mass of MLCC per 1 t of each type of LE used in this study.

3.3. Characterisation of MLCCs from Lighting Equipment via ICP-OES Analysis

The calculated results of concentrations and contents of the examined multi-layer ceramic capacitors are presented in Figure 12. Based on the ICP-OES analysis results (mg L^{-1}), the usable concentrations (mg kg^{-1}) (HNO_3 vs. aqua regia) of rare earth elements and precious metals are presented in Figure 12a. The Sc, Tb, Yb, Lu, and Pt concentrations were out of the quantification limit (OoQL), and the elements Eu, Tm, and Rh were not detected. The corresponding contents (% by weight) are also shown in Figure 12b. The results are a function of the sample specifications and adhesive residues on capacitor terminals. According to [8], MLCCs' ceramic body colour indicates the presence of specific elements in their structures. In particular, brown is associated with Y, red, purple, and blue with Pd, gold, and Ag, and off-white with Ir. The synergy of their chromatic and magnetic separation techniques will create an even more specific recycling flow process.

The sample consisted of different sizes and colours of magnetic capacitors derived from all the lighting equipment used. The percentage of each type of LE in the sample was: LED lamps (domestic use 45.43% and professional use 9.53%), LED luminaires 2.84%, ELEDDCT 3.98%, and LME 38.22%. According to [51,52], dielectric ceramic materials with rare earth element impurities are used in multi-layer ceramic capacitors. Indicatively, in the following studies are mentioned Y [67], La [68], Ce [69], Pr [70], Nd [71], Sm [36], Gd [13], Dy [37], Ho [25], Er [72], Yb [49], and Lu [49]. Apart from the REEs, the presence of PMs was witnessed in the following studies: Au [31,53], Ag [15,31], Ru [57], Pd [22,31], and Ir [8]. As expected, Au's leaching took place only in aqua regia. Ag leaching was 52% higher in

HNO₃, while the leaching of the rest of the precious metals and some rare earth elements was higher in aqua regia (Ru 14.13%, Pd 5.71%, Ir 61.13%, Y 4.86%, La 14.81%, Ce 27.34%, Pr 7.24%, Nd 27.27%, Dy 5.31%, and Er 21.05%). Gd, Ho, and Sm showed small to insignificant differences ranging between 0.40 and 2.10% as a function of the acids used. Due to the nature of the sample, the low concentration of Au may be explained as (a) its main use in electrical–electronic equipment focuses on the internal structure of the integrated circuits and the protection of electrical contacts from environmental conditions such as oxidation; and (b) MLCCs in gold-plated terminals are used in specific and high-cost applications, so their potential presence in the sample is minimal, with external LED drivers and LME being the most likely origin [12,19,73]. Increased concentrations of Ag and Pd may be explained as multi-layer ceramic capacitors being one of the main electrotechnical applications of Ag and, simultaneously, the main electrotechnical application of Pd. Because of this, Pd's concentration in drivers is a function of MLCCs' presence in their electronic circuit.

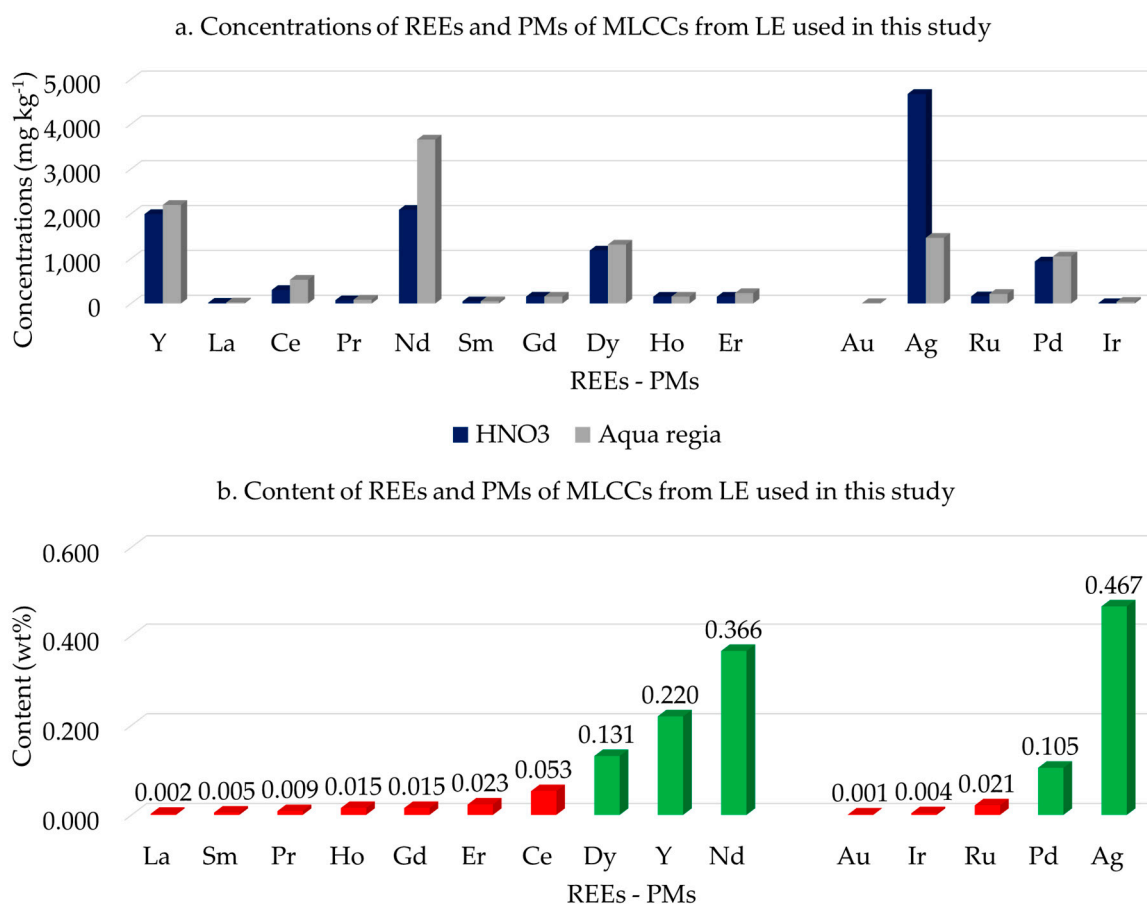


Figure 12. (a). Concentrations of REEs and PMs in MLCCs from LE: HNO₃ vs. aqua regia. (b). Content of REEs and PMs in MLCCs from LE (the red bars correspond to trace elements and the green bars to the main contents).

Also, depending on their composition, the welding residues on the terminals of waste MLCCs form the concentration of Ag [9,15,18]. The authors of [27] report that no Pd was detected in their sample examined via ICP-OES analysis. Considering the highest value among the concentrations of each element, the MLCCs' contents were calculated (Figure 4b). La, Sm, Pr, Ho, Gd, Er, Ce, Au, Ir, and Ru appear as trace elements (content < 0.1%). In contrast, the rest of the investigated elements constitute their main composition. The REE content corresponds to 0.84 wt% and the PM content to 0.60 wt%.

Based on the literature review, the results of the relevant studies, the analytical technique used, and the sample specifications are listed in Tables 2 and 3.

Table 2. Results of analysis based on the literature on the presence or absence of PMs in MLCC structures (wt%).

Au	Ir	Ru	Pd	Ag	Sample's Origin	Analytical Technique	Ref.
<0.0001			1.69		Specific ¹	ICP-OES	[53]
0.01			0.05	0.13	n/a	MP-AES	[21]
			1.24	3.48	n/a	XRF, ICP-MS	[22] *
			1.10	1.99	n/a	SEM-EDS	[24]
					Specific ²	ICP-MS	[8]
			0.5–3		Specific ³	ICP-AES	[45]
			0.14	1.08	Specific ⁴	AAS	[40]
			0.95	5.01	n/a	XRF, ICP-AES	[18,30] *
			0.35	2.02	Specific ⁵	ICP-AES	[26,41] *
<1			<1	(1–20)	n/a	-	[31]
0.001	0.004	0.021	0.105	0.467	Specific ⁶	ICP-OES	Present study

* data on the main composition of MLCCs. ¹ computer, ² MLCCs of specific capacitor colour, ³ non-magnetic MLCCs, ⁴ personal computers, ⁵ Ni-rich MLCCs, and ⁶ Lighting equipment

Table 3. Results of analysis based on the literature on the presence or absence of REEs in MLCC structures (wt%).

La	Sm	Pr	Ho	Gd	Er	Ce	Dy	Y	Nd	Sample's Origin	Analytical Technique	Ref.
								(0.3 & 0.8)		Specific ¹	ICP-MS	[8]
0.002	0.005	0.009	0.015	0.015	0.023	0.053	0.131	0.220	0.366	Specific ²	ICP-OES	Present study

¹ MLCCs of specific capacitor colour, ² Lighting equipment

Some of these studies list the main composition of the rare earth elements and precious metals of the multi-layer ceramic capacitors they used. Differences between the Table 2 and the Table 3 results and this study are possible due to individual or a mix of the following parameters: (a) the WEEE type and category, (b) the brand name, specifications, and manufacture date of equipment, (c) the sample's technology, specifications, and representativeness, and (d) the laboratory process stages and the analytical technique used [8,15,19,25,27,37,74]. This study includes the results on the presence of eleven additional elements to the ones listed below, nine REEs, and two PMs.

Considering the elements' contents, their market prices (Figure A5), and the SR and EI indicators, respectively (Figure A6), as well as the low REE recycling rate (<1%), it is clarified that it is imperative to try to recover even the traces of the critical raw materials contained in the e-waste due to their unique properties, the natural monopoly, environmental protection, and the economic interest [5,75–83].

3.4. EDX Analysis of MLCCs from Lighting Equipment

EDX analysis of the examined multi-layer ceramic capacitors, indicatively presented in Figure 13, confirmed the existence of rare earth elements and precious metals according to [45]. “Standard termination” MLCCs (ST-MLCCs) (Figure 13a) and “flexible termination” MLCCs (FT-MLCCs) (Figure 13b) were found [84,85]. The ST-MLCC terminal's structure (Figure 13(a1)–(a3)) confirmed the presence of BMs and, in particular, tin (Sn), nickel (Ni), and copper (Cu) according to [18,40,41,49].

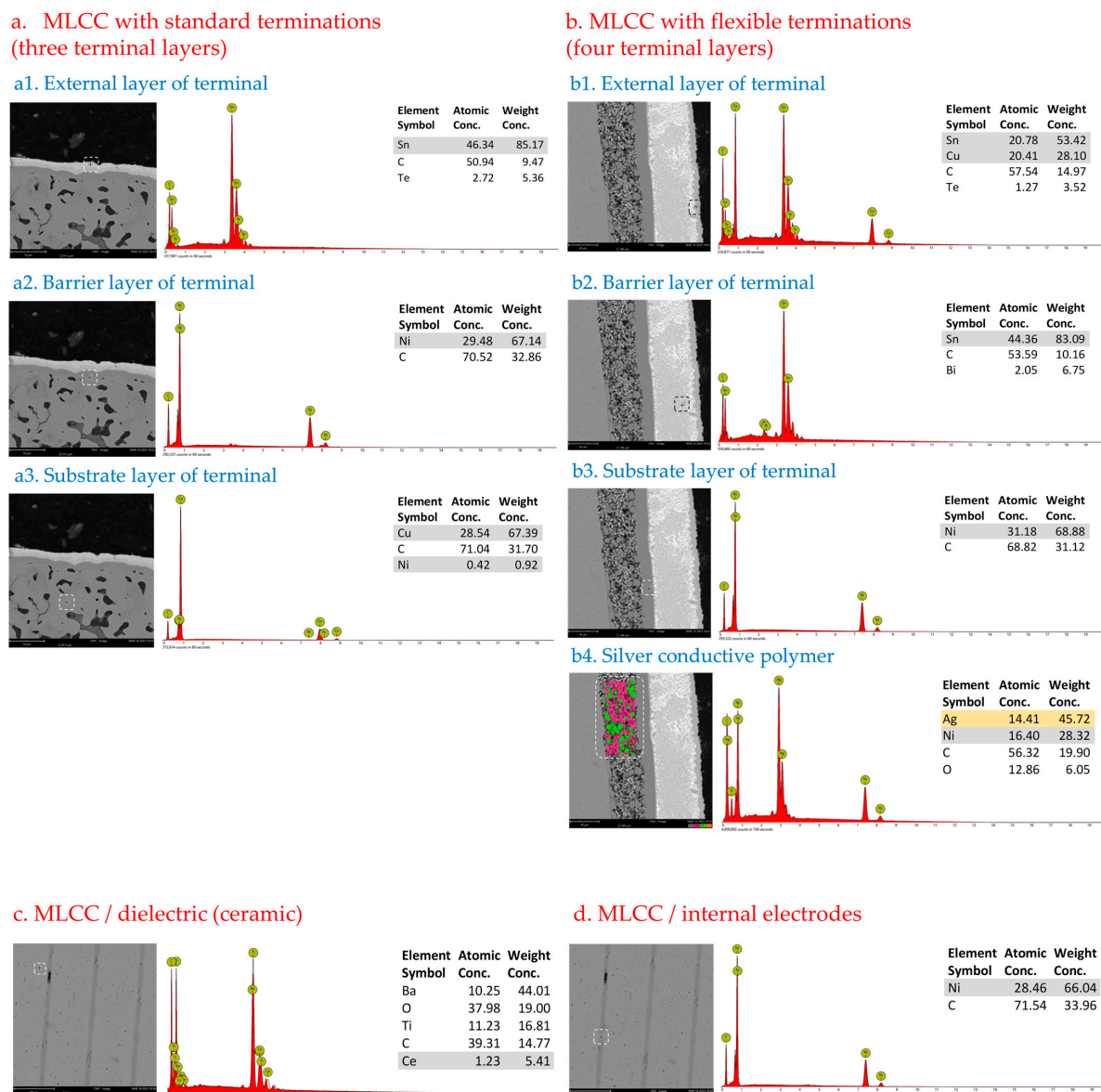


Figure 13. (Authors' images) (a). MLCC with standard terminations/terminal layers (three), (b). MLCC with flexible terminations/terminal layers (four), (c). MLCC/dielectric (ceramic), (d). MLCC/internal electrodes.

Of particular interest was the presence of FT-MLCCs in lighting equipment because they are usually used in equipment of significant cost or in equipment subject to vibrations. Specific materials, such as conductive polymers, were employed before 2008 as an additional (fourth) terminal layer to protect the sensitive ceramic body of multi-layer ceramic capacitors against mechanical stress (Figure 13b). Mechanical stresses are likely to be generated by vibrations due to careless use of the equipment (poor placement or falls), during operation, and as a result of local temperature changes created during the manufacture or repair of drivers. Silver conductive polymer (Figure 13(b4)) aims to absorb the mechanical stress and contribute positively to the equipment's lifetime by protecting the capacitors. From the recycling point of view, this additional layer contributes to the concentration of Ag [37,49,85].

Ce, barium (Ba), and titanium (Ti) were detected in the ceramic dielectric (Figure 13c), and Ni was detected in electrodes (Figure 13d). Precious metals were not detected in their electrodes, even though Pt and a Ag–Pd alloy (70–30) were used for their manufacture [16,22,42,43,49,69].

The REE–PM content of the examined multi-layer ceramic capacitors by ICP-OES corresponds to 1.44 wt%; therefore, 98.56 wt% corresponds to BMs, TMs, and ceramic dielectrics.

According to the literature, this significant percentage by weight may include the following elements with their respective percentages of the total mass of the MLCCs (Figure 14a), their market price (Figure 14b), as well as a graph of the SR index and a comparison with REEs and PMs (Figure 14c): Sn 1–5.7%, Cu 1.76–8%, Ni 0.68–66.1%, Ba 17.4–48.65%, Ti 11.4–19.36%, lead (Pb) 1.03–8.82%, bismuth (Bi) 0.18–0.66%, iron (Fe) 3.71%, zinc (Zn) 0.19%, manganese (Mn) 0.23%, aluminium (Al) 0.15%, chromium (Cr) 0.31%, and niobium (Nb) 3.48% [18,21,22,26,27,30,40,41,43].

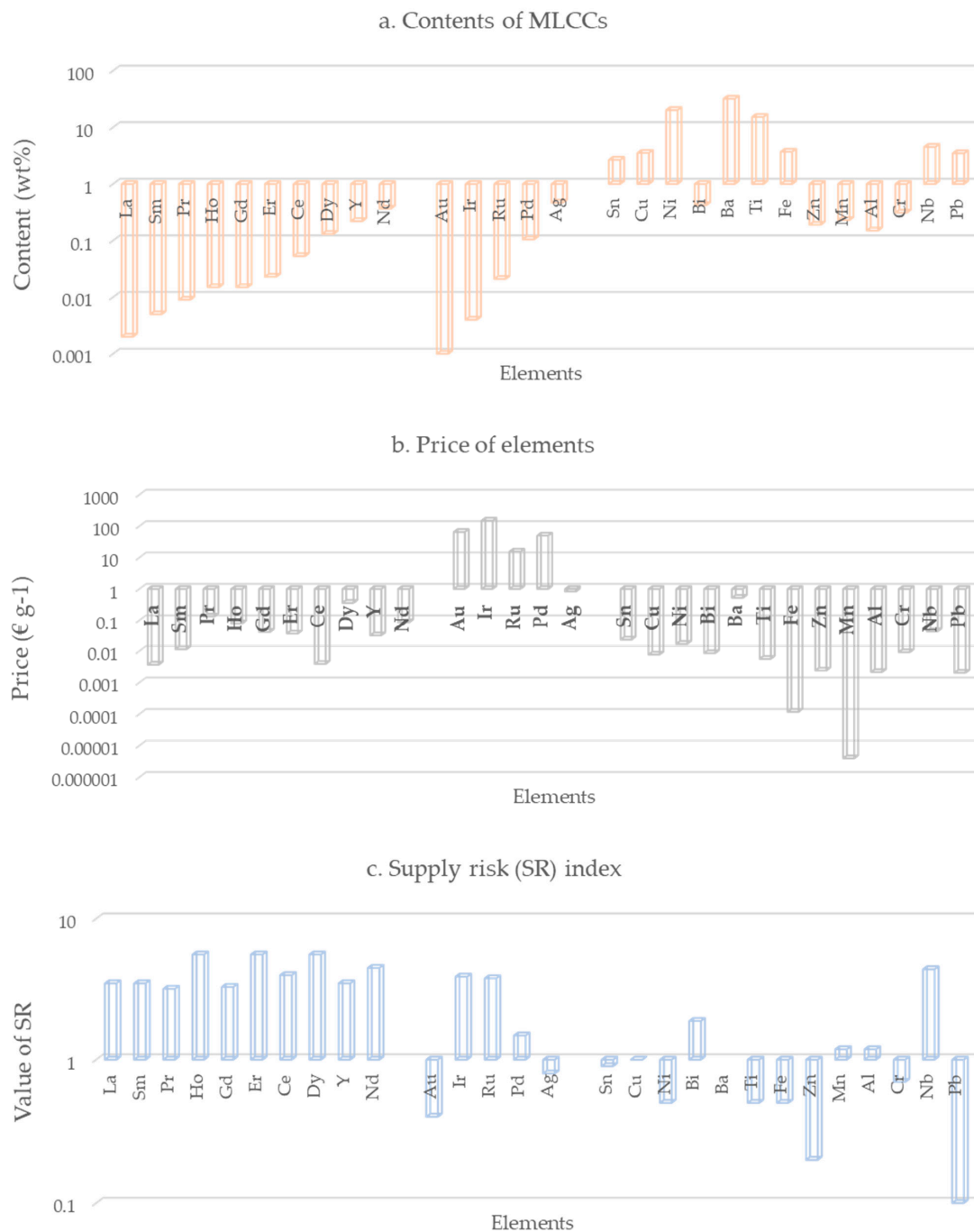


Figure 14. Comparative diagram of the contents of MLCCs, the values of the elements that may be contained in their structure, and the SR index for these elements.

Based on the comparative diagrams, it can be understood that the REEs cover the CRMs, whereas the PMs cover both the criticality of their components and the economic benefit of the recycling of the MLCCs. Some PMs' Au, Pd, and Ag elements may have comparable SR values to other elements such as Bi and Nb. However, they differ significantly in their high economic value.

4. MLCCs as Target Components and Their Store Value

Ideal futuristic recycling is related to the individual characterisation of e-waste structures and components and their separate recycling [3]. All concentrations of the examined multi-layer ceramic capacitors were significantly higher than those of the Earth's crust, while the excluding elements (La, Sm, Pr, Ho, Gd, and Er) are also higher than in natural mining [86]. Critical raw materials are located in specific structures or components of electrical–electronic equipment [87]. For both MLCCs, SMD-LEDs, and tantalum capacitors (TCs), scientific interest exists in their separate recycling because of their CRM and TM contents. Comparing their concentrations about specific elements (Figure 15) shows that multi-layer ceramic capacitors lag significantly behind in Au and Y, are comparable for Ag, and outperform significantly for Ce and Gd. It is worth noting that the literature review shows that SMD-LEDs and TCs do not contain Pd [8,74,87–97].

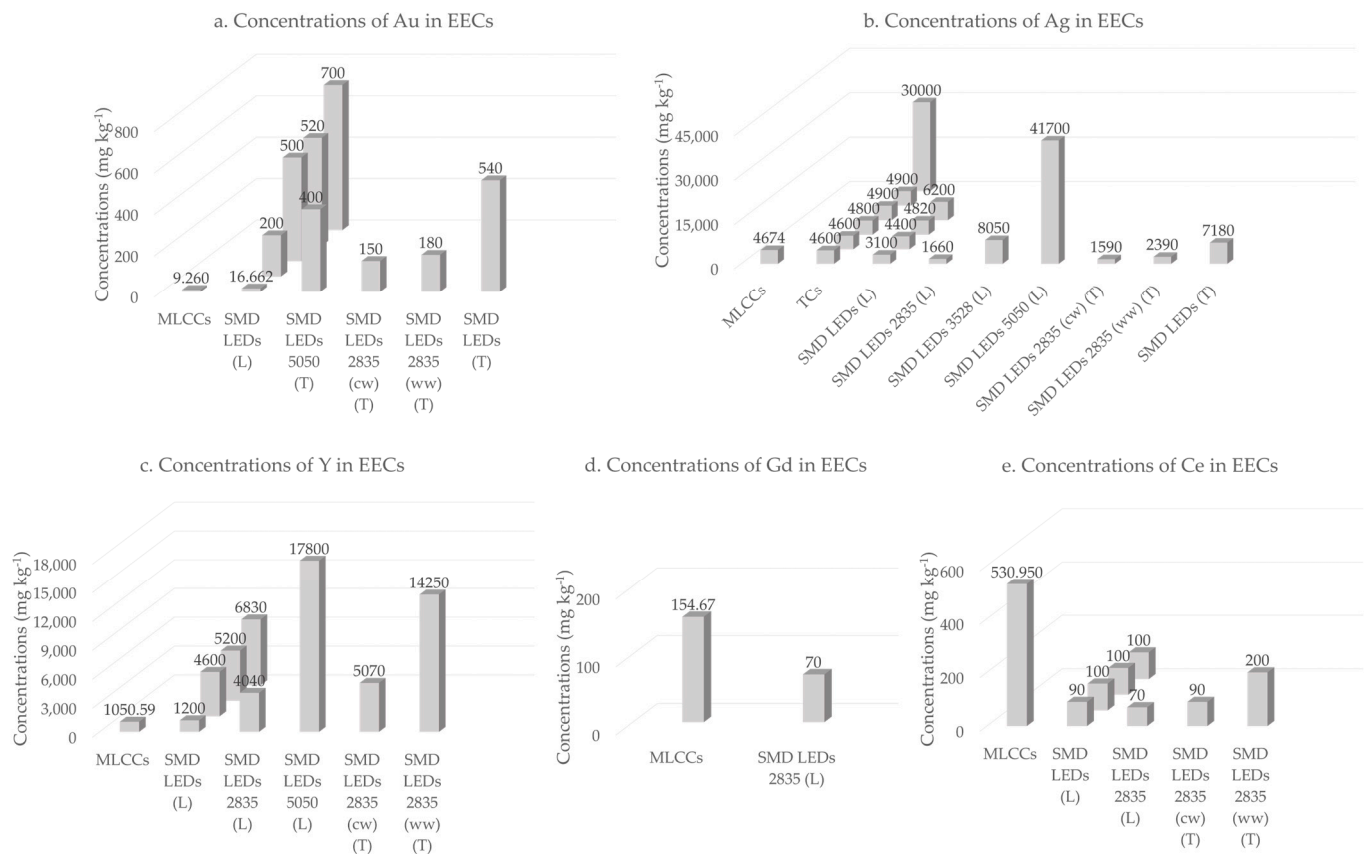


Figure 15. Comparison between concentrations of the examined MLCCs used in this study, different types of SMD-LEDs, and TCs.

The calculation and distribution of the stored value for an assumed mass of 1 kg of multi-layer ceramic capacitors from lighting equipment due to the presence of rare earth elements and precious metals was performed considering only their usable concentrations and current market prices. The results are presented in a Sankey diagram (Figure 16), where extremely low participation in the REE stored value was observed. At the same time, the dominant participation of Pd is highlighted. The stored value of these metals has a significant economic impact ($\sim 67 \text{ EUR kg}^{-1}$), which is essentially created by precious

metals at a rate of 98.67%, with Pd leading the way in its configuration (Au 0.90%, Ag 5.82%, Ru 4.94%, Pd 78.37%, and Ir 8.64%).

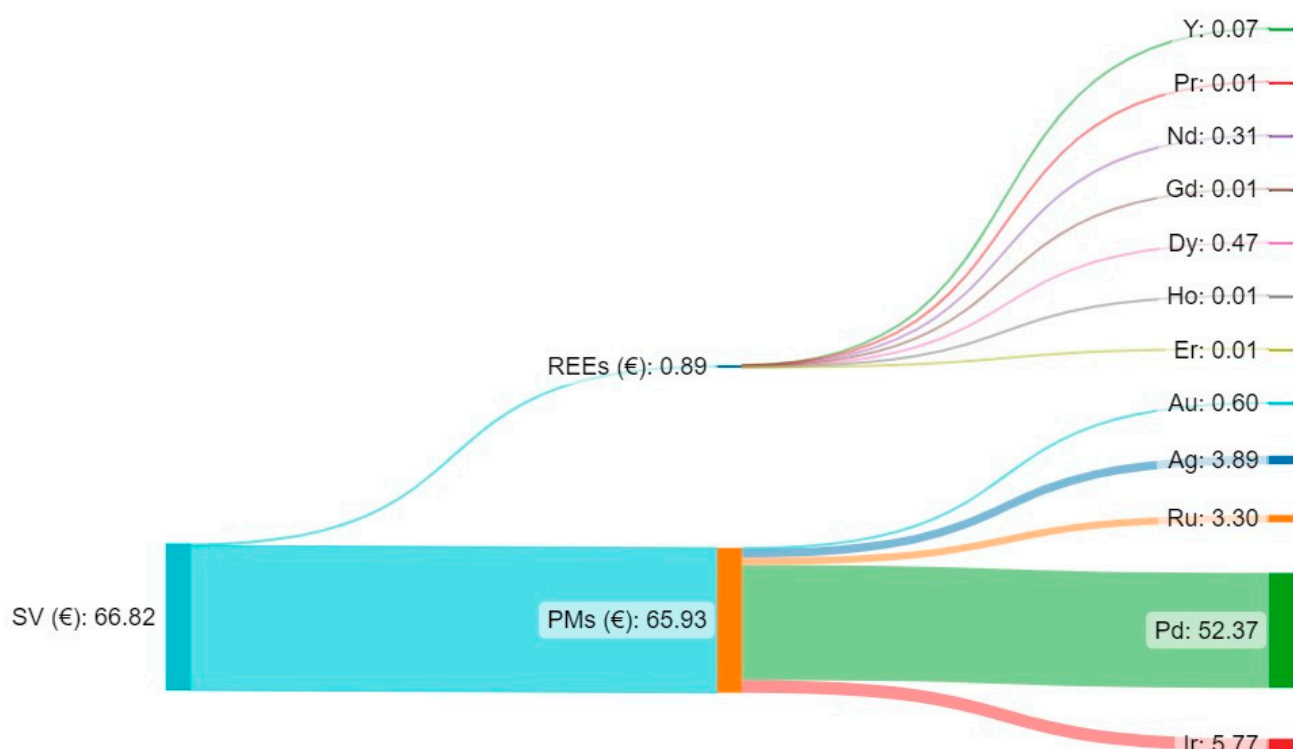


Figure 16. Sankey diagram of stored value in MLCCs of mass 1 kg due to the presence of REEs and PMs (EUR) (made with SankeyMATIC).

It is worth noting that the high concentration of Ag combined with its low market price (Figure A5) of 0.84 (EUR g^{−1}) and the low concentration of Ru combined with its high market price of 15.5 (EUR g^{−1}) form a similar level of participation in the stored value. Correspondingly, the exceptionally high market price of Ir 149.5 (EUR g^{−1}) compensates for its extremely low concentration, creating a remarkable contribution. According to [21], in their economic–technical analysis for a mass of 1 kg of multi-layer ceramic capacitors from waste PCBs, the modulation of the overall stored value from precious metals corresponded to 81.4% (Ag 3.8%, Au 20.4%, and Pd 57.2%), while the remaining percentage corresponded to the following data, which also contribute to the formation of the total stored value of multi-layer ceramic capacitors: Ti 7.2%, Ni 7.5%, and the rest (Cu, Zn, Mn, Al, Sn, Ba, and Pb) at 3.94%. The synergy of chromatic and magnetic separation techniques of capacitors of this type may create even more specific recycling flow processes with significant changes in their stored economic value, contributing to the sustainability of recycling plants [8].

5. Conclusions

The continuous increase in e-waste is a complex problem that requires special handling. Critical raw materials are found in their specific structures and components, which usually provide the ability to separate and recycle them. Multi-layer ceramic capacitors, due to their elemental composition, are of particular interest for their separate recycling. Sorting them based on their magnetic properties and colour can create recycling flows of specific critical raw materials, which will contribute to protecting the environment and natural reserves, partial independence from the “monopoly” of these metals, and the sustainability of recycling plants.

The presence of MLCCs in the examined types of lighting equipment corresponded to 83% (15 out of 18 types), and the probability of their presence in these 15 types ranged between 12.5 and 100%. Their average total mass per examined lighting equipment type

ranged between 0.033 and 0.328 g, while their average mass per examined multi-layer ceramic capacitor as a function of lighting equipment type ranged between 0.011 and 0.196 g. The participation of Category 3 WEEE was extremely low compared with the other five categories. Still, it consists only of lamps, particularly the type G9-C, which is the most essential type for collecting MLCCs among the examined lighting equipment with a performance of ~ 17 (kg t⁻¹) (per ton of each type of lighting equipment) compared with the other types whose performance ranged between 65 and 1640 g.

In the MLCCs used in this study, ten RREs and five PMs were detected with the content of 0.84 wt% and 0.60 wt%, respectively, which creates an SV equal to 66.82 (EUR kg⁻¹) with Pd dominating with 78.37%. Their main composition concerns the elements Dy 0.131 wt%, Y 0.220 wt%, Nd 0.366 wt%, Pd 0.105 wt%, and Ag 0.467 wt%, while the elements La, Sm, Pr, Ho, Gd, Er, Ce, Au, Ir, and Ru are shown based on their contents as trace elements and with a content ranging between 0.001 wt% and 0.053 wt%.

Expanding the use of MLCCs with flexible terminations versus MLCCs with standard terminations in driver manufacturing may reduce the growth rate of WEEE through EEE protection and contribute positively to the stored value of the drivers.

The idea of recycling a particular type of electrical or electronic waste is confirmed or rejected by the e-waste characterisation studies and their results. However, the feasibility and viability of recycling facilities will be determined by the efforts to recover these specific elements of the periodic table, in particular CRMs and precious metals.

The results suggest (a) their selective conditional removal and (b) their separate recycling.

Author Contributions: Conceptualization, K.M.S.; methodology, K.M.S., D.F. and V.N.S.; validation, P.S.; formal analysis, K.M.S., D.F. and V.N.S.; investigation, K.M.S.; resources, K.M.S., D.F. and V.N.S.; data curation, K.M.S., D.F. and V.N.S.; writing—original draft preparation, K.M.S.; writing—review and editing, K.M.S.; visualization, K.M.S. and P.S.; supervision, P.S.; project administration, P.S.; funding acquisition, K.M.S. All authors have read and agreed to the published version of the manuscript.

Funding: This research received no external funding.

Data Availability Statement: The data presented in this study are available on request from the corresponding author.

Acknowledgments: Special thanks go to: 1. the recycling company “AEGEAN RECYCLING-FOUNDRIES S.A.” for supplying LED materials (lamps, luminaires, and drivers), 2. Venetia Dikaiopoulou from FEILO SYLVANIA GREECE S.A. for her contribution to the supply of LED lamps, 3. Nikolaos Spanidis ABB for his contribution to the supply of LME materials, 4. Evangelos Vasilopoulos, SIEMENS Greece, for his contribution to the supply of LME materials, 5. Ioanna Kyriopoulou from the Laboratory of Materials and Environmental Chemistry P.P.C. S.A. for the assistance with the use of equipment, ICP-OES analysis of samples, and useful discussions, and 6. Christina Skoulikidou, Vassilis Orfanos, Aristidis Stenos, and Konstantinos Liogas for useful discussions. The authors K. Sideris, D. Fragoulis, V. Stathopoulos, and P. Siniros acknowledge the financial support for the dissemination of this work from the Special Account for Research of ASPETE through the funding program “Strengthening ASPETE’s research”.

Conflicts of Interest: The authors declare that they have no known competing financial interest or personal relationships that could have influenced the work reported in this study.

Nomenclature

BMEs	Base Metal Electrodes
BMs	Base Metals
BMs-MLCCs	Base Metal Multi-Layer Ceramic Capacitors
BN	Brand Name
CRMs	Critical Raw Materials
EECs	Electrical–Electronic Components

EEE	Electrical–Electronic Equipment
EI	Economic Importance
EU	European Union
e-waste	Electronic waste
FT-MLCCs	Flexible Termination Multi-Layer Ceramic Capacitors
ICP-AES	Inductively Coupled Plasma Atomic Emission Spectroscopy
ICP-MS	Inductively Coupled Plasma Mass Spectrometry
ICP-OES	Inductively Coupled Plasma Optical Emission Spectroscopy
LE	Lighting Equipment
LED	Light-Emitting Diode
MLCCs	Multi-Layer Ceramic Capacitors
MP-AES	Microwave Plasma Atomic Emission Spectroscopy
MpP	Mass per Piece
OoQL	Out of Quantification Limit
PCB	Printed Circuit Board
PGMs	Platinum Group Metals
PMs	Precious Metals
REEs	Rare Earth Elements
SEM-EDS	Scanning Electron Microscopy Energy Dispersive Spectroscopy
SEM-EDX	Scanning Electron Microscopy Energy Dispersive X-ray (Spectroscopy)
SMD LEDs	Surface Mount Device Light Emitting Diodes
SMD-EECs	Surface Mount Device Electrical Electronics Components
SMD-MLCCs	Surface Mount Device Multi-Layer Ceramic Capacitors
SMDs	Surface Mount Devices
SR	Supply Risk
ST-MLCCs	Standard Termination Multi-Layer Ceramic Capacitors
TCs	Tantalum Capacitors
TEM-EDXS	Transmission Electron Microscopy Energy-Dispersive X-ray Spectroscopy
TGA	Thermogravimetric Analysis
THCs	Through-Hole Components
TMs	Technological Metals
WEEE	Waste Electrical–Electronic Equipment
XRF	X-ray Fluorescence

Appendix A

Indexes for lighting equipment used in this study	
Index C	Classic {LED lamps with SMD LEDs (e.g., E27-C)} – plus on the type of LE
Index R	Retro {LED lamps with filament LEDs (e.g., E27-R)} – plus on the type of LE

Colour code for lighting equipment used in this study		
Type of LE	Colour code	Description
E27-C		LED lamps
E14-C		LED lamps
G9-C		LED lamps
R7S-C		LED lamps
GU10		LED lamps
MR16		LED lamps
E27-R		LED lamps
E14-R		LED lamps
E27-C-P		LED lamps (Professional use)
GU10-C-P		LED lamps (Professional use)
LEDT (T8)		LED lamps (Tubes 8) (Professional use)
LEDLD		LED Luminaires (Downlight) (Professional use)
LEDLP		LED Luminaires (Professional use)
ELEDDCT		External Light Emitting Diodes Drivers Closed Type
LME		Light Management Equipment (domestic & professional use)

Figure A1. Colour code for LE.

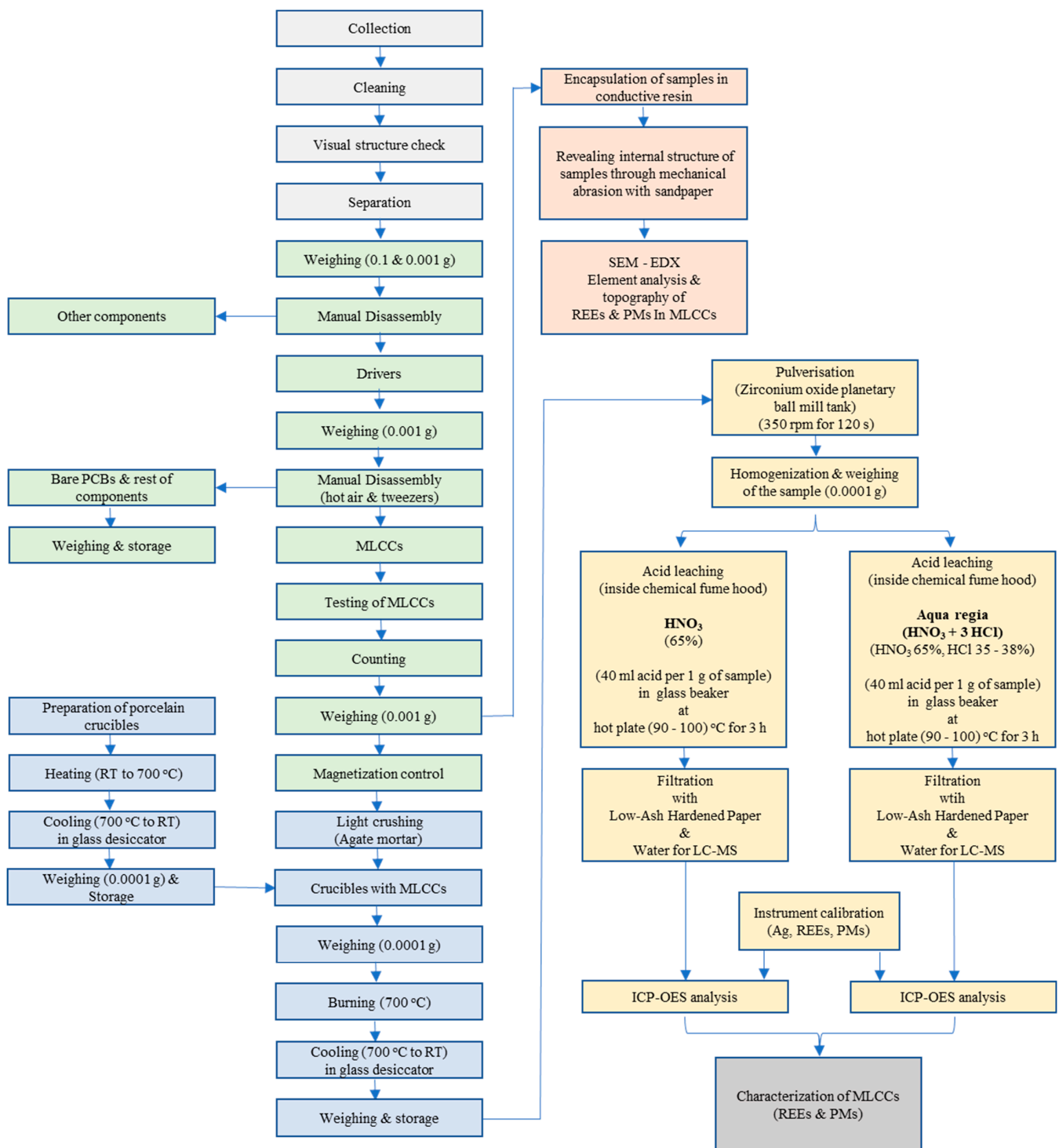


Figure A2. Supervisory flow chart, from sample collection to analysis.

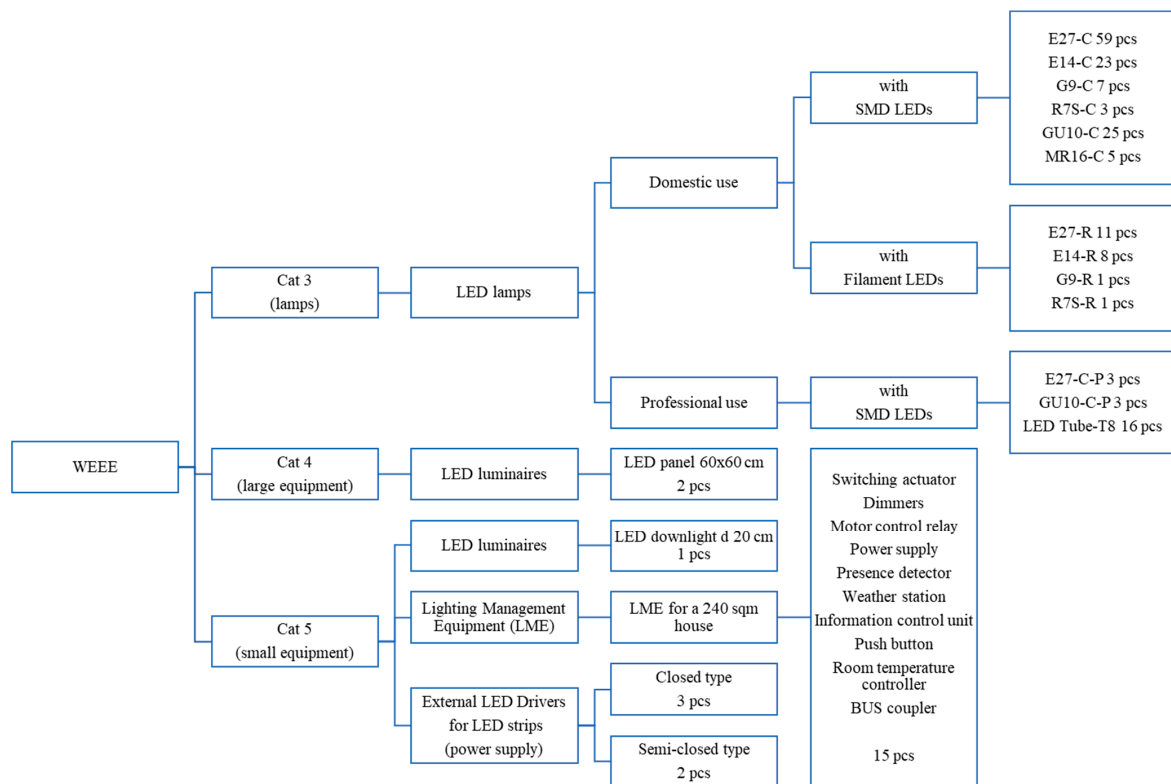


Figure A3. Separation of LE according to WEEE categories, domestic or professional use, and surface mount device (SMD) or filament.

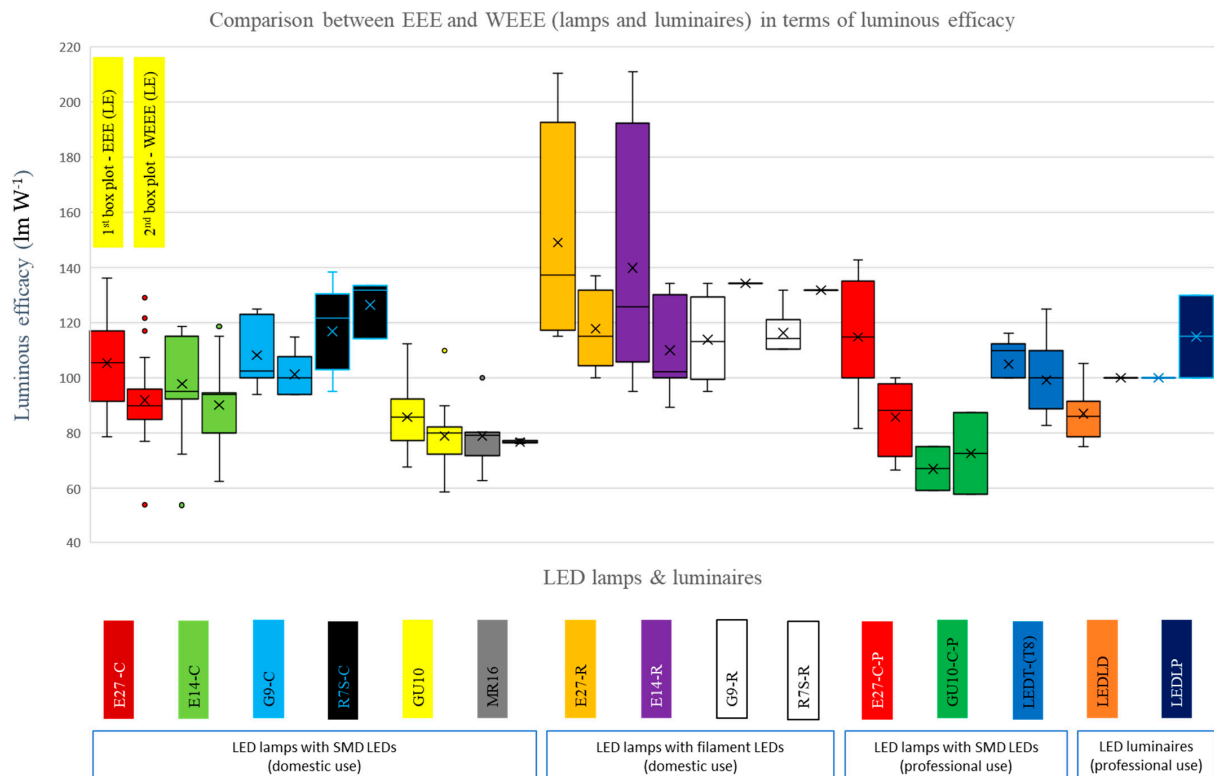


Figure A4. Matching the efficiency (lm W^{-1}) of LED technology lamps and luminaires to estimate the manufacturing date of the equipment examined in this study.

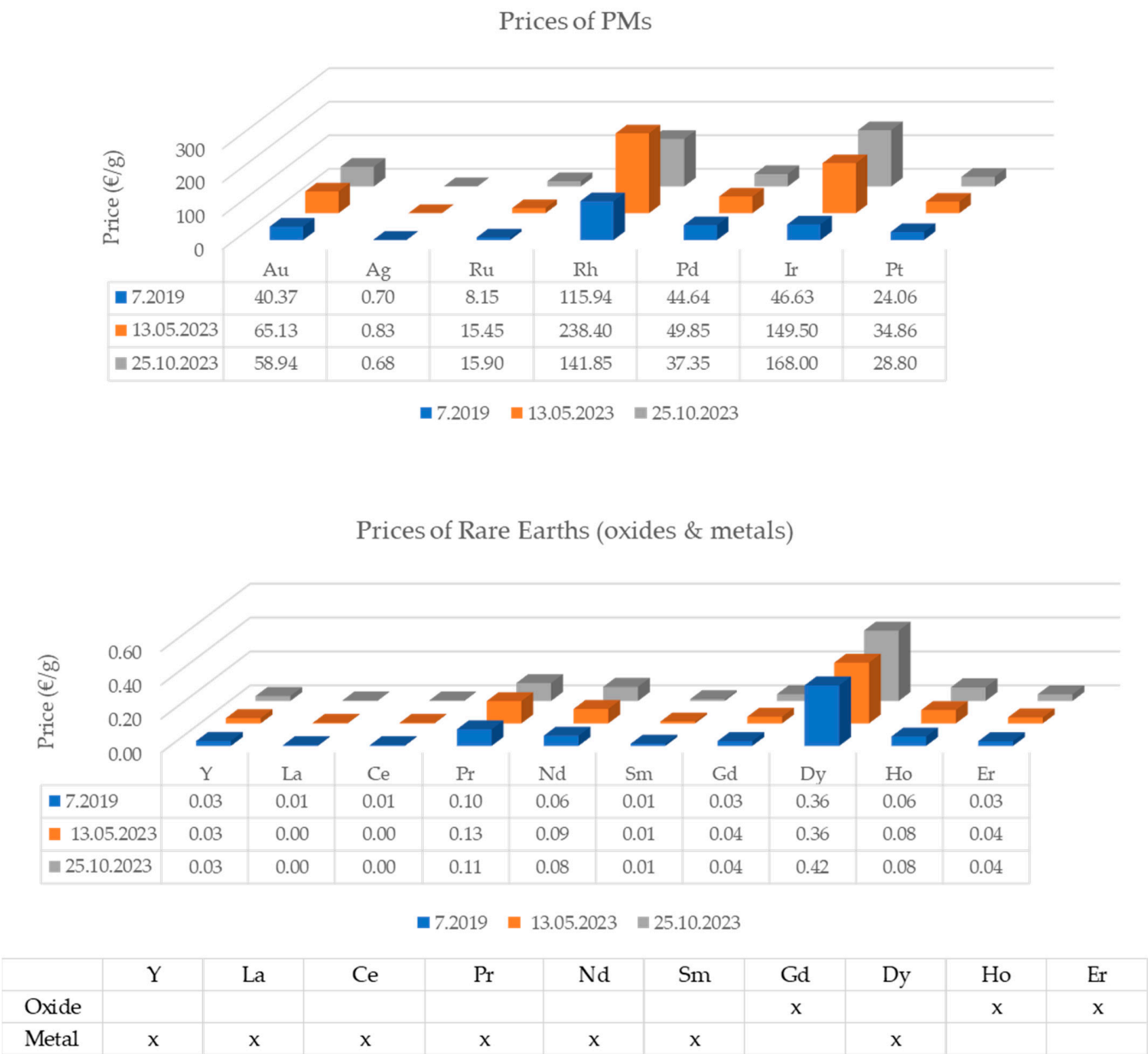


Figure A5. Prices of elements.

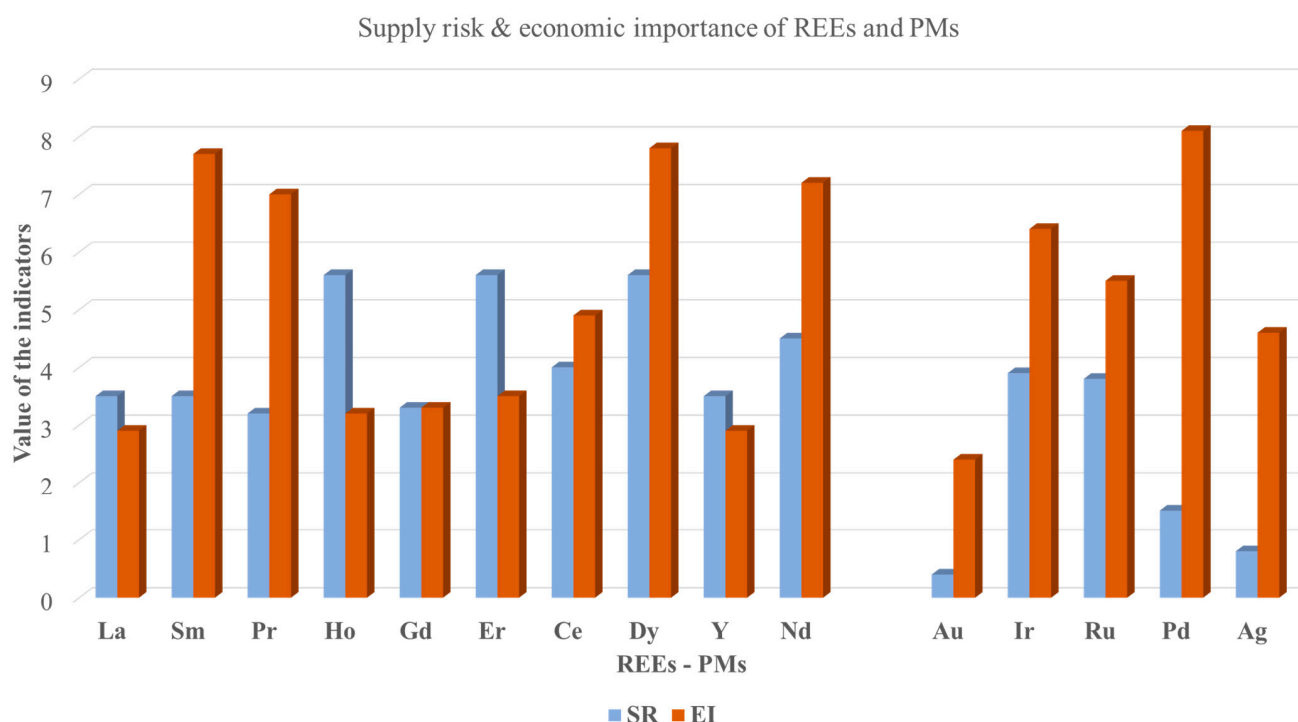


Figure A6. Supply Risk (SR) and Economic Importance (EI) indexes.

References

- Birloaga, I.; Coman, V.; Kopacek, B.; Vegliò, F. An advanced study on the hydrometallurgical processing of waste computer printed circuit boards to extract their valuable content of metals. *Waste Manag.* **2014**, *34*, 2581–2586. [\[CrossRef\]](#)
- Di Piazza, S.; Cecchi, G.; Cardinale, A.M.; Carbone, C.; Mariotti, M.G.; Giovine, M.; Zotti, M. Penicillium expansum Link strain for a biometallurgical method to recover REEs from WEEE. *Waste Manag.* **2017**, *60*, 596–600. [\[CrossRef\]](#)
- Mir, S.; Dhawan, N. A comprehensive review on the recycling of discarded printed circuit boards for resource recovery. *Resour. Conserv. Recycl.* **2022**, *178*, 106027. [\[CrossRef\]](#)
- Kaya, M. Recovery of metals and nonmetals from electronic waste by physical and chemical recycling processes. *Waste Manag.* **2016**, *57*, 64–90. [\[CrossRef\]](#)
- European Commission. *Study on the Critical Raw Materials for the EU*; European Commission: Brussels, Belgium, 2023. [\[CrossRef\]](#)
- Wani, S.; Majeed, S. Rare-Earth nanomaterials for Bio-Probe applications. *Appl. Biol. Res.* **2017**, *19*, 241. [\[CrossRef\]](#)
- Cardoso, C.E.D.; Almeida, J.C.; Lopes, C.B.; Trindade, T.; Vale, C.; Pereira, E. Recovery of Rare Earth Elements by Carbon-Based Nanomaterials—A Review. *Nanomaterials* **2019**, *9*, 814. [\[CrossRef\]](#)
- Charles, R.G.; Douglas, P.; Dowling, M.; Liversage, G.; Davies, M.L. Towards Increased Recovery of Critical Raw Materials from WEEE—evaluation of CRMs at a component level and pre-processing methods for interface optimisation with recovery processes. *Resour. Conserv. Recycl.* **2020**, *161*, 104923. [\[CrossRef\]](#)
- Maurice, A.A.; Dinh, K.N.; Charpentier, N.M.; Brambilla, A.; Gabriel, J.-C.P. Dismantling of printed circuit boards enabling electronic components sorting and their subsequent treatment open improved elemental sustainability opportunities. *Sustainability* **2021**, *13*, 10357. [\[CrossRef\]](#)
- Gidakos, E.; Akcil, A. WEEE under the prism of urban mining. *Waste Manag.* **2020**, *102*, 950–951. [\[CrossRef\]](#)
- Van Yken, J.; Boxall, N.J.; Cheng, K.Y.; Nikoloski, A.N.; Moheimani, N.R.; Kaksonen, A.H. E-waste recycling and resource recovery: A review on technologies, barriers and enablers with a focus on oceania. *Metals* **2021**, *11*, 1313. [\[CrossRef\]](#)
- Gautam, P.; Behera, C.K.; Sinha, I.; Gicheva, G.; Singh, K.K. High added-value materials recovery using electronic scrap-transforming waste to valuable products. *J. Clean. Prod.* **2022**, *330*, 129836. [\[CrossRef\]](#)
- Alam, M.A.; Zuga, L.; Pecht, M.G. Economics of rare earth elements in ceramic capacitors. *Ceram. Int.* **2012**, *38*, 6091–6098. [\[CrossRef\]](#)
- Binnemans, K.; Jones, P.T. Perspectives for the recovery of rare earths from end-of-life fluorescent lamps. *J. Rare Earths* **2014**, *32*, 195–200. [\[CrossRef\]](#)
- Charles, R.G.; Douglas, P.; Hallin, I.L.; Matthews, I.; Liversage, G. An investigation of trends in precious metal and copper content of RAM modules in WEEE: Implications for long term recycling potential. *Waste Manag.* **2017**, *60*, 505–520. [\[CrossRef\]](#)
- Smith, L.; Ibn-Mohammed, T.; Koh, S.C.L.; Reaney, I.M. Life cycle assessment and environmental profile evaluations of high volumetric efficiency capacitors. *Appl. Energy* **2018**, *220*, 496–513. [\[CrossRef\]](#)

17. de la Torre, E.; Vargas, E.; Ron, C.; Gámez, S. Europium, yttrium, and indium recovery from electronic wastes. *Metals* **2018**, *8*, 777. [\[CrossRef\]](#)
18. Liu, Y.; Zhang, L.; Song, Q.; Xu, Z. Recovery of palladium and silver from waste multilayer ceramic capacitors by eutectic capture process of copper and mechanism analysis. *J. Hazard. Mater.* **2020**, *388*, 122008. [\[CrossRef\]](#)
19. Silva, L.H.d.S.; Júnior, A.A.F.; Azevedo, G.O.A.; Oliveira, S.C.; Fernandes, B.J.T. Estimating recycling return of integrated circuits using computer vision on printed circuit boards. *Appl. Sci.* **2021**, *11*, 2808. [\[CrossRef\]](#)
20. Milinovic, J.; Rodrigues, F.J.L.; Barriga, F.J.A.S.; Murton, B.J. Ocean-Floor Sediments as a Resource of Rare Earth Elements: An Overview of Recently Studied Sites. *Minerals* **2021**, *11*, 142. [\[CrossRef\]](#)
21. Prabakaran, G.; Barik, S.P.; Kumar, B. A hydrometallurgical process for recovering total metal values from waste monolithic ceramic capacitors. *Waste Manag.* **2016**, *52*, 302–308. [\[CrossRef\]](#)
22. Niu, B.; Xu, Z. Application of Chloride Metallurgy and Corona Electrostatic Separation for Recycling Waste Multilayer Ceramic Capacitors. *ACS Sustain. Chem. Eng.* **2017**, *5*, 8390–8395. [\[CrossRef\]](#)
23. Zhou, J.; Zhu, N.; Liu, H.; Wu, P.; Zhang, X.; Zhong, Z. Recovery of gallium from waste light emitting diodes by oxalic acidic leaching. *Resour. Conserv. Recycl.* **2019**, *146*, 366–372. [\[CrossRef\]](#)
24. Niu, B.; Xu, Z. Innovating e-waste recycling: From waste multi-layer ceramic capacitors to Nb–Pb codoped and ag–Pd–Sn–Ni loaded BaTiO₃ nano-photocatalyst through one-step ball milling process. *Sustain. Mater. Technol.* **2019**, *21*, e00101. [\[CrossRef\]](#)
25. Hernández, V.I.; García-Gutiérrez, D.I.; Aguilar-Garib, J.A.; Nava-Quintero, R.J. Characterization of precipitates formed in X7R 0603 BME-MLCC during sintering. *Ceram. Int.* **2021**, *47*, 310–319. [\[CrossRef\]](#)
26. Liu, Y.; Song, Q.; Zhang, L.; Xu, Z. Separation of metals from Ni–Cu–Ag–Pd–Bi–Sn multi-metal system of e-waste by leaching and stepwise potential-controlled electrodeposition. *J. Hazard. Mater.* **2021**, *408*, 124772. [\[CrossRef\]](#) [\[PubMed\]](#)
27. Xu, J.; Liu, D.; Lee, C.; Feydi, P.; Chapuis, M.; Yu, J.; Billy, E.; Yan, Q.; Gabriel, J.C.P. Efficient Electrocatalyst Nanoparticles from Upcycled Class II Capacitors. *Nanomaterials* **2022**, *12*, 2697. [\[CrossRef\]](#)
28. Buechler, D.T.; Zyaykina, N.N.; Spencer, C.A.; Lawson, E.; Ploss, N.M.; Hua, I. Comprehensive elemental analysis of consumer electronic devices: Rare earth, precious, and critical elements. *Waste Manag.* **2020**, *103*, 67–75. [\[CrossRef\]](#)
29. Fischer, A.C.; Forsberg, F.; Lapisa, M.; Bleiker, S.J.; Stemme, G.; Roxhed, N.; Niklaus, F. Integrating MEMS and ICs. *Microsystems Nanoeng.* **2015**, *1*, 15005. [\[CrossRef\]](#)
30. Liu, Y.; Song, Q.; Zhang, L.; Xu, Z. Behavior of enrichment and migration path of Cu–Ag–Pd–Bi–Pb in the recovery of waste multilayer ceramic capacitors by eutectic capture of copper. *J. Clean. Prod.* **2021**, *287*, 125469. [\[CrossRef\]](#)
31. Wu, C.; Awasthi, A.K.; Qin, W.; Liu, W.; Yang, C. Recycling value materials from waste PCBs focus on electronic components: Technologies, obstruction and prospects. *J. Environ. Chem. Eng.* **2022**, *10*, 108516. [\[CrossRef\]](#)
32. Kumari, R.; Samadder, S.R. A critical review of the pre-processing and metals recovery methods from e-wastes. *J. Environ. Manage.* **2022**, *320*, 115887. [\[CrossRef\]](#) [\[PubMed\]](#)
33. Xia, D.; Charpentier, N.M.; Maurice, A.A.; Brambilla, A.; Yan, Q.; Gabriel, J.-C.P. Sustainable route for Nd recycling from waste electronic components featured with unique element-specific sorting enabling simplified hydrometallurgy. *Chem. Eng. J.* **2022**, *441*, 135886. [\[CrossRef\]](#)
34. Charpentier, N.M.; Maurice, A.A.; Xia, D.; Li, W.-J.; Chua, C.-S.; Brambilla, A.; Gabriel, J.-C.P. Urban mining of unexploited spent critical metals from E-waste made possible using advanced sorting. *Resour. Conserv. Recycl.* **2023**, *196*, 107033. [\[CrossRef\]](#)
35. Kadota, M.; Shoji, H.; Hatakeyama, A.; Wada, K. Output current ripple reduction of LED driver using ceramic-capacitor-input circuit and buck-boost converter. *Electr. Eng. Jpn. Engl. Transl. Denki Gakkai Ronbunshi* **2019**, *209*, 26–34. [\[CrossRef\]](#)
36. Hernández-López, A.M.; Aguilar-Garib, J.A.; Guillemet-Fritsch, S.; Nava-Quintero, R.; Dufour, P.; Tenaillon, C.; Durand, B.; Valdez-Nava, Z. Reliability of X7R multilayer ceramic capacitors during High Accelerated Life Testing (HALT). *Materials* **2018**, *11*, 1900. [\[CrossRef\]](#) [\[PubMed\]](#)
37. Huang, C.M.; Romero, J.A.; Osterman, M.; Das, D.; Pecht, M. Life cycle trends of electronic materials, processes and components. *Microelectron. Reliab.* **2019**, *99*, 262–276. [\[CrossRef\]](#)
38. Pankaj Kumar Electronic waste–hazards, management and available green technologies for remediation—A review. *Int. Res. J. Environ. Sci.* **2018**, *7*, 57–68.
39. Sarvar, M.; Salarirad, M.M.; Shabani, M.A. Characterization and mechanical separation of metals from computer Printed Circuit Boards (PCBs) based on mineral processing methods. *Waste Manag.* **2015**, *45*, 246–257. [\[CrossRef\]](#)
40. Panda, R.; Dinkar, O.S.; Jha, M.K.; Pathak, D.D. Hydrometallurgical processing of waste multilayer ceramic capacitors (MLCCs) to recover silver and palladium. *Hydrometallurgy* **2020**, *197*, 105476. [\[CrossRef\]](#)
41. Liu, Y.; Song, Q.; Zhang, L.; Xu, Z. Novel approach of in-situ nickel capture technology to recycle silver and palladium from waste nickel-rich multilayer ceramic capacitors. *J. Clean. Prod.* **2021**, *290*, 125650. [\[CrossRef\]](#)
42. Fu, Y.; Hou, Y.; Song, B.; Cheng, H.; Liu, X.; Yu, X.; Zheng, M.; Zhu, M. Construction of lead-free dielectrics for high temperature multilayer ceramic capacitors and its inner electrode matching characteristics. *J. Alloys Compd.* **2022**, *903*, 163995. [\[CrossRef\]](#)
43. Liu, X.; Hou, Y.; Song, B.; Cheng, H.; Fu, Y.; Zheng, M.; Zhu, M. Lead-free multilayer ceramic capacitors with ultra-wide temperature dielectric stability based on multifaceted modification. *J. Eur. Ceram. Soc.* **2022**, *42*, 973–980. [\[CrossRef\]](#)
44. Andrade, D.F.; Castro, J.P.; Garcia, J.A.; Machado, R.C.; Pereira-Filho, E.R.; Amarasiwardena, D. Analytical and reclamation technologies for identification and recycling of precious materials from waste computer and mobile phones. *Chemosphere* **2022**, *286*, 131739. [\[CrossRef\]](#) [\[PubMed\]](#)

45. Bourgeois, D.; Lacanau, V.; Mastretta, R.; Contino-Pépin, C.; Meyer, D. A simple process for the recovery of palladium from wastes of printed circuit boards. *Hydrometallurgy* **2020**, *191*, 105241. [CrossRef]
46. Mizuno, Y.; Kishi, H.; Ohnuma, K.; Ishikawa, T.; Ohsato, H. Effect of site occupancies of rare earth ions on electrical properties in Ni-MLCC based on BaTiO₃. *J. Eur. Ceram. Soc.* **2007**, *27*, 4017–4020. [CrossRef]
47. Shen, Z.; Wang, X.; Gong, H.; Wu, L.; Li, L. Effect of MnO₂ on the electrical and dielectric properties of Y-doped Ba_{0.95}Ca_{0.05}Ti_{0.85}Zr_{0.15}O₃ ceramics in reducing atmosphere. *Ceram. Int.* **2014**, *40*, 13833–13839. [CrossRef]
48. Gong, H.; Wang, X.; Zhang, S.; Li, L. Synergistic effect of rare-earth elements on the dielectric properties and reliability of BaTiO₃-based ceramics for multilayer ceramic capacitors. *Mater. Res. Bull.* **2016**, *73*, 233–239. [CrossRef]
49. Teverovsky, A. Cracking Problems in Low-Voltage Chip Ceramic Capacitors. In *NASA Electronic Parts and Packaging Program*; NASA Goddard Space Flight Center: Greenbelt, MD, USA, 2018; pp. 1–73.
50. Hong, K.; Lee, T.H.; Suh, J.M.; Yoon, S.H.; Jang, H.W. Perspectives and challenges in multilayer ceramic capacitors for next generation electronics. *J. Mater. Chem. C* **2019**, *7*, 9782–9802. [CrossRef]
51. Patil, R.P.; Hiragond, C.; Jain, G.H.; Khanna, P.K.; Gaikwad, V.B.; More, P.V. La doped BaTiO₃ nanostructures for room temperature sensing of NO₂/NH₃: Focus on La concentration and sensing mechanism. *Vacuum* **2019**, *166*, 37–44. [CrossRef]
52. Dash, T.; Mohapatra, S.S.; Mishra, R.K.; Palei, B.B. Synthesis and analysis of structural properties of (Ba_{0.592}Sr_{0.0406})TiO₃ compound. *Mater. Today Proc.* **2020**, *43*, 362–365. [CrossRef]
53. Delfini, M.; Ferrini, M.; Manni, A.; Massacci, P.; Piga, L.; Scoppettuolo, A. Optimization of Precious Metal Recovery from Waste Electrical and Electronic Equipment Boards. *J. Environ. Prot.* **2011**, *02*, 675–682. [CrossRef]
54. Shanthi Bhavan, J.; Joy, J.; Pazhani, A. Identification and recovery of rare earth elements from electronic waste: Material characterization and recovery strategies. *Mater. Today Commun.* **2023**, *36*, 106921. [CrossRef]
55. Laubertova, M.; Malindzakova, M.; Trpcevska, J.; Gajić, N. Assessment of sampling and chemical analysis of waste printed circuit boards from weee: Gold content determination. *Metall. Mater. Eng.* **2019**, *25*, 171–182. [CrossRef] [PubMed]
56. Kaliyaraj, D.; Rajendran, M.; Angamuthu, V.; Antony, A.R.; Kaari, M.; Thangavel, S.; Venugopal, G.; Joseph, J.; Manikkam, R. Bioleaching of heavy metals from printed circuit board (PCB) by *Streptomyces albidoflavus* TN10 isolated from insect nest. *Bioresour. Bioprocess.* **2019**, *6*, 47. [CrossRef]
57. Bobnar, V.; Hrovat, M.; Holc, J.; Kosec, M. All-Ceramic Percolative Composites with a Colossal Dielectric Response. In *Ferroelectrics—Characterization and Modeling*; IntechOpen: London, UK, 2011. [CrossRef]
58. International Energy Agency. Available online: <https://www.iea.org/data-and-statistics/charts/global-lighting-sales-historical-and-in-the-net-zero-scenario-2010-2030> (accessed on 1 May 2023).
59. KAFKAS. kafkas.gr. Available online: <https://www.kafkas.gr/lambes/led/> (accessed on 1 May 2023).
60. Sim, J.-K.; Ashok, K.; Ra, Y.-H.; Im, H.-C.; Baek, B.-J.; Lee, C.-R. Characteristic enhancement of white LED lamp using low temperature co-fired ceramic-chip on board package. *Curr. Appl. Phys.* **2012**, *12*, 494–498. [CrossRef]
61. Gago Calderón, A.; Narvarte Fernández, L.; Carrasco Moreno, L.M.; Serón Barba, J. LED bulbs technical specification and testing procedure for solar home systems. *Renew. Sustain. Energy Rev.* **2015**, *41*, 506–520. [CrossRef]
62. De Santi, C.; Dal Lago, M.; Buffolo, M.; Monti, D.; Meneghini, M.; Meneghesso, G.; Zanoni, E. Failure causes and mechanisms of retrofit LED lamps. *Microelectron. Reliab.* **2015**, *55*, 1765–1769. [CrossRef]
63. Dillon, H.E.; Ross, C.; Dzombak, R. Environmental and Energy Improvements of LED Lamps over Time: A Comparative Life Cycle Assessment. *LEUKOS* **2018**, *16*, 229–237. [CrossRef]
64. Richter, J.L.; Tähkämö, L.; Dalhammar, C. Trade-offs with longer lifetimes? The case of LED lamps considering product development and energy contexts. *J. Clean. Prod.* **2019**, *226*, 195–209. [CrossRef]
65. Wehbie, M.; Semetey, V. Characterization of end-of-life LED lamps: Evaluation of reuse, repair and recycling potential. *Waste Manag.* **2022**, *141*, 202–207. [CrossRef]
66. Liu, D.D. NASA Electronic Parts and Packaging Program Selection, Qualification, Inspection, and Derating of Multilayer Ceramic Capacitors with Base-Metal Electrodes. 2013. Available online: https://nepp.nasa.gov/files/24396/EEE_Parts_Bulletin_Apr-May2013_final.pdf (accessed on 20 April 2023).
67. Tihtih, M.; Ibrahim, J.E.F.M.; Basyooni, M.A.; En-Nadir, R.; Belaid, W.; Hussainova, I.; Kocserha, I. Development of Yttrium-Doped BaTiO₃ for Next-Generation Multilayer Ceramic Capacitors. *ACS Omega* **2023**, *8*, 8448–8460. [CrossRef] [PubMed]
68. Zhang, W.; Yang, J.; Wang, F.; Chen, X.; Mao, H. Enhanced dielectric properties of La-doped 0.75BaTiO₃-0.25Bi(Mg_{0.5}Ti_{0.5})O₃ ceramics for X9R-MLCC application. *Ceram. Int.* **2021**, *47*, 4486–4492. [CrossRef]
69. Lakov, L.; Aleksandrova, M.; Blaskov, V. Current trends in the development of high dielectric permittivity ceramics. *Mater. Sci. Non-Equilib. Phase Transform.* **2020**, *10*, 8–10.
70. Duan, R.; Wang, J.; Jiang, S.; Cheng, H.; Li, J.; Song, A.; Hou, B.; Chen, D.; Liu, Y. Impact of La doping on performance of Na_{0.5}Bi_{0.5}TiO₃-Ba_{0.7-x}LaxSr_{0.3}Sn_{0.1}Ti_{0.9-0.25x}O₃ dielectric ceramics. *J. Alloys Compd.* **2018**, *745*, 121–126. [CrossRef]
71. Sasikumar, S.; Thirumalaisamy, T.K.; Saravanakumar, S.; Asath Bahadur, S.; Sivaganesh, D.; Shameem Banu, I.B. Effect of neodymium doping in BaTiO₃ ceramics on structural and ferroelectric properties. *J. Mater. Sci. Mater. Electron.* **2020**, *31*, 1535–1546. [CrossRef]
72. Paunović, V.; Mitić, V.V.; Đorđević, M.; Marjanović, M.; Kocić, L. Electrical characteristics of Er doped BaTiO₃ ceramics. *Sci. Sinter.* **2017**, *49*, 129–137. [CrossRef]

73. MLCC Gold Termination. Available online: <https://www.kyocera-avx.com/products/ceramic-capacitors/surface-mount/mlcc-gold-termination-au-series/> (accessed on 10 April 2023).
74. Andooz, A.; Egbalpour, M.; Kowsari, E.; Ramakrishna, S.; Cheshmeh, Z.A. A comprehensive review on pyrolysis of E-waste and its sustainability. *J. Clean. Prod.* **2022**, *333*, 130191. [CrossRef]
75. Costis, S.; Mueller, K.K.; Coudert, L.; Neculita, C.M.; Reynier, N.; Blais, J.F. Recovery potential of rare earth elements from mining and industrial residues: A review and cases studies. *J. Geochem. Explor.* **2021**, *221*, 106699. [CrossRef]
76. Brewer, A.; Dohnalkova, A.; Shutthanandan, V.; Kovarik, L.; Chang, E.; Sawvel, A.M.; Mason, H.E.; Reed, D.; Ye, C.; Hynes, W.F.; et al. Microbe Encapsulation for Selective Rare-Earth Recovery from Electronic Waste Leachates. *Environ. Sci. Technol.* **2019**, *53*, 13888–13897. [CrossRef]
77. Ueberschaar, M.; Geiping, J.; Zamzow, M.; Flamme, S.; Rotter, V.S. Assessment of element-specific recycling efficiency in WEEE pre-processing. *Resour. Conserv. Recycl.* **2017**, *124*, 25–41. [CrossRef]
78. Institute for Rare Earths and Strategic Metals. Available online: https://ise-metal-quotes.com/?gclid=EAIaIQobChMlz-zCy53y_gIVHYCDBx3B1gDJEAAAYAAAEglv1_D_BwE (accessed on 13 May 2023).
79. Metal Prices. Available online: <https://pmm.unicore.com/en/prices/> (accessed on 13 May 2023).
80. Precious Metals. Available online: <https://www.macrotrends.net/charts/precious-metals> (accessed on 25 October 2023).
81. Bullion by Post. Available online: <https://www.bullionbypost.eu/gold-price> (accessed on 25 October 2023).
82. Platinum Group Metals Market Reports. Available online: <https://www.sfa-oxford.com/platinum-group-metals/pgm-market-reports> (accessed on 25 October 2023).
83. Rare Earth Elements—Statistics & Facts. Available online: <https://www.statista.com/topics/1744/rare-earth-elements/#topicOverview> (accessed on 15 April 2023).
84. Keimasi, M.; Azarian, M.H.; Pecht, M. Isothermal aging effects on flex cracking of multilayer ceramic capacitors with standard and flexible terminations. *Microelectron. Reliab.* **2007**, *47*, 2215–2225. [CrossRef]
85. Vogel, G. Avoiding flex cracks in ceramic capacitors: Analytical tool for a reliable failure analysis and guideline for positioning cercaps on PCBs. *Microelectron. Reliab.* **2015**, *55*, 2159–2164. [CrossRef]
86. Bookhagen, B.; Bastian, D.; Buchholz, P.; Faulstich, M.; Oppel, C.; Irrgeher, J.; Prohaska, T.; Koeberl, C. Metallic resources in smartphones. *Resour. Policy* **2020**, *68*, 101750. [CrossRef]
87. Cenci, M.P.; Dal Berto, F.C.; Castillo, B.W.; Veit, H.M. Precious and critical metals from wasted LED lamps: Characterization and evaluation. *Environ. Technol.* **2020**, *43*, 1870–1881. [CrossRef] [PubMed]
88. Niu, B.; Chen, Z.; Xu, Z. Recovery of Valuable Materials from Waste Tantalum Capacitors by Vacuum Pyrolysis Combined with Mechanical–Physical Separation. *ACS Sustain. Chem. Eng.* **2017**, *5*, 2639–2647. [CrossRef]
89. Niu, B.; Chen, Z.; Xu, Z. Application of pyrolysis to recycling organics from waste tantalum capacitors. *J. Hazard. Mater.* **2017**, *335*, 39–46. [CrossRef]
90. Chen, Z.; Niu, B.; Zhang, L.; Xu, Z. Vacuum pyrolysis characteristics and parameter optimization of recycling organic materials from waste tantalum capacitors. *J. Hazard. Mater.* **2018**, *342*, 192–200. [CrossRef]
91. Zhan, L.; Xia, F.; Ye, Q.; Xiang, X.; Xie, B. Novel recycle technology for recovering rare metals (Ga, In) from waste light-emitting diodes. *J. Hazard. Mater.* **2015**, *299*, 388–394. [CrossRef]
92. Dodbiba, G.; Oshikawa, H.; Ponou, J.; Kim, Y.; Haga, K.; Shibayama, A.; Fujita, T. Treatment of Spent LED Light Bulbs for Recycling of Its Components: A Combined Assessment in the Context of LCA and Cost-Benefit Analysis. *Resour. Process.* **2019**, *66*, 15–28. [CrossRef]
93. Cenci, M.P.; Berto, F.C.D.; Schneider, E.L.; Veit, H.M. Assessment of LED lamps components and materials for a recycling perspective. *Waste Manag.* **2020**, *107*, 285–293. [CrossRef]
94. Zhan, L.; Wang, Z.; Zhang, Y.; Xu, Z. Recycling of metals (Ga, In, As and Ag) from waste light-emitting diodes in sub/supercritical ethanol. *Resour. Conserv. Recycl.* **2020**, *155*, 104695. [CrossRef]
95. Oliveira, R.P.; Botelho Junior, A.B.; Espinosa, D.C.R. Characterization of Wasted LEDs from Tubular Lamps Focused on Recycling Process by Hydrometallurgy. In *Energy Technology 2020: Recycling, Carbon Dioxide Management, and Other Technologies*; Springer International Publishing: Cham, Switzerland, 2020; pp. 317–325. [CrossRef]
96. Vinhal, J.T.; de Oliveira, R.P.; Coleti, J.L.; Espinosa, D.C.R. Characterization of end-of-life LEDs: Mapping critical, valuable and hazardous elements in different devices. *Waste Manag.* **2022**, *151*, 113–122. [CrossRef] [PubMed]
97. Niu, B.; Chen, Z.; Xu, Z. Method for recycling tantalum from waste tantalum capacitors by chloride metallurgy. *ACS Sustain. Chem. Eng.* **2017**, *5*, 1376–1381. [CrossRef]

Disclaimer/Publisher’s Note: The statements, opinions and data contained in all publications are solely those of the individual author(s) and contributor(s) and not of MDPI and/or the editor(s). MDPI and/or the editor(s) disclaim responsibility for any injury to people or property resulting from any ideas, methods, instructions or products referred to in the content.